

3. RADIATION MEASUREMENTS

U.S. Department of Energy
201 Varick Street, 5th Floor
New York, NY 10014-4811

	<u>Page</u>
3. Radiation Measurements	3.1-1
3.1 Overview	3.1-1
3.2 Ionization Chambers	3.2-1
3.2.1 Scope	3.2-1
3.2.2 PIC System Design	3.2-1
3.2.2.1 Ion Chamber	3.2-1
3.2.2.2 Electrometer	3.2-2
3.2.2.3 Readout Systems	3.2-3
3.2.3 Data Analysis	3.2-3
3.2.4 Calibration	3.2-4
3.2.5 Inferring Exposure (Dose) Rate	3.2-6
3.3 Field Gamma-Ray Spectrometry	3.3-1
3.3.1 Scope	3.3-1
3.3.2 Instrumentation	3.3-2
3.3.3 Site Selection and Instrument Setup	3.3-3
3.3.4 Calibration	3.3-4
3.3.5 Spectrum Analysis	3.3-8
3.3.6 Inventory Measurements	3.3-10
3.3.6.1 Application	3.3-10
3.3.6.2 Homogeneous Terrain	3.3-11
3.3.6.3 Nonhomogeneous Terrain	3.3-12
3.3.7 Spectral Stripping for Germanium Detectors	3.3-14
3.3.7.1 Application	3.3-14
3.3.7.2 Theory	3.3-14
3.3.7.3 Determination of Stripping Parameters (f and r)	3.3-15
3.3.7.4 Stripping Operation	3.3-16

	<u>Page</u>
3.3.8 Sodium Iodide Detectors	3.3-17
3.3.8.1 Application	3.3-17
3.3.8.2 Equipment	3.3-17
3.3.8.3 Peak Analysis	3.3-18
3.3.8.4 Energy Band Analysis	3.3-18
3.3.8.5 Total Spectrum Energy Analysis	3.3-20
 3.4 Remote Gamma-Ray Spectrometry Stations	 3.4-1
3.4.1 Scope	3.4-1
3.4.2 Components	3.4-2
3.4.3 Instrumentation Assembly	3.4-3
3.4.4 EML Quality Control	3.4-5
 3.5 Thermoluminescence Dosimetry	 3.5-1
3.5.1 Scope	3.5-1
3.5.2 Special Apparatus	3.5-1
3.5.3 Predeployment Preparation of Chips	3.5-4
3.5.4 Environmental Deployment	3.5-5
3.5.5 Readout and Calibration	3.5-6
3.5.6 Analysis of Results	3.5-7
 3.6 Bonner-Sphere Neutron Spectrometry	 3.6-1
3.6.1 Scope	3.6-1
3.6.2 General Description	3.6-1
3.6.3 Personnel and Training	3.6-2
3.6.4 Methodology	3.6-2
3.6.4.1 Description of the System	3.6-2
3.6.4.2 The Bonner Spheres	3.6-3
3.6.4.3 The Response Functions	3.6-3

	<u>Page</u>
3.6.4.4 Calibrations	3.6-3
3.6.4.5 Electronics	3.6-4
3.6.5 Neutron Spectrum Unfolding	3.6-4
3.6.6 Acceptable Solution	3.6-5

3. *RADIATION MEASUREMENTS*

3.1 OVERVIEW

Since about 1950, the Environmental Measurements Laboratory has carried out major research programs directed at the study of ionizing radiation and natural and man-made radionuclides in the working and in the public environment. Among these studies have been: (1) the long-term investigation of the atmospheric distribution and ground deposition of radionuclides from global fallout generated by nuclear weapons tests; (2) the evaluation of the radiation exposure of human populations from these nuclides as well as those deposited locally by the Nevada weapons tests, those released from nuclear facilities (including the reactor accidents at Three Mile Island and Chernobyl), and those normally present from natural sources; and (3) the determination of radiation worker exposures at particle accelerators, nuclear reactors, and other nuclear facilities. An important component of these studies has been the development and improvement of techniques for low-level radiation measurement and data interpretation. In the following sections, five highly generic measurement systems are described that have been developed and/or refined at EML, and that have found wide application in environmental radiation studies. In each case, an essential part of the system is the methodology associated with detector calibration, measurement procedure(s), and data analysis and interpretation. The indicated references provide additional details and examples of applications for the interested reader.

3.2 IONIZATION CHAMBERS

Contact Person(s) : Kevin M. Miller

3.2.1 SCOPE

This section describes the design, analysis procedures, calibration, and use of pressurized ionization chambers (PIC). These instrument systems are used at EML in the assessment of the penetrating component (gamma plus cosmic-ray secondaries) of the environmental radiation field. Accurate and highly precise measurements of the total exposure rate (or dose rate in air) are made of such sources as:

1. cosmic-ray secondary radiation (high energy muons, photons, and electrons) in the lower atmosphere;
2. natural background radiation from primordial radionuclides (and progeny) in the soil and air;
3. anthropogenic isotopes associated with
 - a. direct radiation from nuclear facilities,
 - b. gaseous effluents from nuclear operations,
 - c. fallout deposition,
 - d. residual radioactivity at sites undergoing clean-up.

3.2.2 PIC SYSTEM DESIGN

3.2.2.1

ION CHAMBER

The chamber selected as our standard consists of a 25-cm diameter stainless-steel sphere with a wall thickness of 2.37 g cm⁻² filled to a pressure of 2.5 MPa (25 atmospheres) with ultrapure argon gas. The collecting electrode is a 5-cm diameter hollow

sphere at the center of the chamber supported by a 0.6-cm diameter rod, which in turn is connected to the chamber shell at the center of a triaxial metal-ceramic seal. The middle conductor of this seal serves as a guard ring and is kept at true circuit ground. A 300-V battery is used to provide bias to the outer shell. This voltage along with the large center electrode results in complete charge collection in fields of up to $10 \mu\text{Gy h}^{-1}$.

Smaller versions of this chamber are also routinely used. They consist of an 18-cm diameter sphere with the same or slightly thicker wall and filling pressures of up to 3.7 MPa. The collecting electrode for these chambers measures 1.9-cm in diameter. Complete charge collection has been observed at $400 \mu\text{Gy h}^{-1}$ with a bias of 300 V.

A complete description of experimental and theoretical investigations involving various PIC designs can be found in De Campo et al. (1972). Known commercial suppliers of these PICs are GE Reuter-Stokes (Twinsburg, Ohio 44087) and LND, Inc. (Oceanside, New York 11572).

3.2.2.2

ELECTROMETER

The ion current from the PIC is measured with a temperature compensated electrometer consisting of a MOSFET (metal oxide semiconductor field effect transistor) and an operational amplifier using 100% negative feedback from the amplifier output to the MOSFET input (Negro et al., 1974). Stable voltage regulators, external to the electrometer, are used to provide power. The electrometer itself is small and light enough to attach directly to the triaxial connector on the PIC and suspend freely without additional support. This arrangement minimizes mechanical stress on the seal insulators and any resultant piezo-electric currents. The response to radiation is about 3 fA per nGy h^{-1} for the large 2.5 MPa chambers and about half that for the 3.7 MPa small chambers. A glass encapsulated tera-ohm carbon resistor used in the feedback loop of the electrometer determines the output sensitivity, generally about 3 mV per nGy h^{-1} , and time response, generally on the order of a few seconds. The electrometer saturates at somewhat over 5 V, which translates to about 1700 nGy h^{-1} .

3.2.2.3 **READOUT SYSTEMS**

Direct observation of the electrometer output voltage is made with a standard voltmeter. To obtain precise measurements, signal integration is performed by one of two methods listed below.

A. Survey mode.

For real-time results, a voltage-to-frequency converter with scaler and calibrated digital readout is used to provide readings with selectable integration times of 4, 40, or 400 sec. This readout system is generally used with the 18-cm diameter chambers in the form of a two-unit package called a SPICER (small pressurized ionization chamber for environmental radiation; Latner et al., 1983). The system is battery powered and can be either held in hand or tripod mounted. Figure 3.1 shows the system in this latter mode of operation.

B. Monitor mode.

The second read-out method is designed for continuous remote monitoring. It consists of an analog to digital converter, timing and control circuitry, and a magnetic tape cassette recorder (Memodyne, Model 201) housed in a weather proof aluminum box (Cassidy et al., 1974). The ion chamber and electrometer are packaged in a similar box which sits atop the recorder box during operation in the field as shown in Figure 3.2. The standard system records the digitized electrometer output voltage every 10 sec, and is capable of storing up to 17 days of data on a single cassette. Some units have been modified to allow the option of recording every 10, 20 or 40 sec. An alkaline cell battery pack provides power for 8 weeks of operation.

3.2.3 **DATA ANALYSIS**

The magnetic tape cassette is read out with a Memodyne 3122 ABV reader interfaced to a Hewlett-Packard 9826 computer using a specially developed analysis program (Gogolak, 1982). The analysis procedure is as follows:

1. A 6 h record of the 10-sec data is read into the computer and displayed on a screen.
2. The data is averaged over 5-min intervals, corrected for the zero reading of the electrometer and converted to exposure rate via a chamber specific calibration factor.
3. A printout of the 5-min averages as well as the average over each hour is made. The standard deviation (SD) of the 5-min data for each hour is also computed and printed.
4. Subsequent 6-h records are analyzed and at the end of the tape a summary plot of the hourly data is made. Bad data sections are then edited and a final printout and plot of the corrected hourly average and SD data is obtained. The hourly average maximum and minimum and daily average are also printed for each day along with the average over the entire period.
5. Permanent storage of the corrected 5-min data is made on a diskette.
6. If desired, the data can be analyzed for any dose due to the passage of a plume (Gogolak and Miller, 1974). The analysis routine examines the SD of the 5-min data in each hour and if it is sufficiently high ($> 1.7 \text{ nGy h}^{-1}$) it is assumed that a fluctuating plume component was present. A search is then made on each side of the plume hour for the nearest three background hours indicated by a standard deviation that is sufficiently low ($< 1 \text{ nGy h}^{-1}$). The average background is computed from these 6 h and subtracted from the total dose in the plume hour to yield the net plume dose.

3.2.4 CALIBRATION

Calibration of the PIC is performed using a National Institute of Standards and Technology (NIST) certified sealed 37 MBq ^{226}Ra source and a shadow shield technique (De Campo et al., 1972). The shadow shield method is necessary because it removes the contribution of the room scatter component which we have found to be on the order of 30% of that from the primary beam. At the same time, it also corrects for any other constant factors included in the PIC output such as room background, electrometer zero offset, and α and stress currents. The calibration procedure is as follows:

1. The source is placed in a low mass holder at a height of about 1 m above the floor and at a distance of 4, 5, or 6 m to the PIC (geometric center), which is at the same height on a low mass stand.
2. A 30-cm thick lead shield with a cross section measuring 10-x-10 cm is interposed on a low mass stand so as to intercept all primary rays from the source to all parts of the PIC through the full thickness of the shield. Alignment is checked with a string with a dummy source in place. Slight overshielding (a larger shadow) on the order of 1-2 cm is used as this results in a negligible error as opposed to undershielding which could produce a significant error. The use of a shield with a cross section that is roughly half that of the PIC is recommended because the shadow size cast will require the shield to be placed near the midpoint between the source and the PIC thus minimizing the production and interception of lead fluorescent X-rays and also allowing a proper alignment which is not too critical to shield placement.
3. The source is placed in its holder and the output signal of the PIC is averaged over a 10- to 30-min time period.
4. The lead shield is removed (leaving its stand in place so as to change the scattering conditions as little as possible), and the PIC output signal is averaged again over a 10- to 30-min period.
5. The difference between the average signals (reading with shield not in place minus reading with shield in place) is divided by the exposure rate delivered by the source at that distance to yield the Ra primary beam calibration factor. This calibration factor must be adjusted by a small amount for the energy spectrum that will be encountered for a particular radiation field. For our standard 25 cm-2.5 MPa chamber, this correction yields a 3% higher sensitivity for a normal background radiation field, while for the 18 cm-3.7 MPa chamber it is 1% higher.
6. Background readings are taken in the calibration room and in a whole body counter in both the negative and positive high voltage modes of operation to verify that the system does not have stress currents present and that there is no high internal background.

3.2.5 INFERRING EXPOSURE (DOSE) RATE

The total PIC current can be expressed as

$$R = k_c I_c + k_t I_t + R'$$

where

- k_c = the calibration factor for cosmic radiation
- I_c = the cosmic radiation exposure rate
- k_t = the calibration factor for terrestrial radiation
- I_t = the terrestrial radiation exposure rate
- R' = the α particle current from contamination in the steel shell (~2 fA for the 25-cm chamber and 1 fA for the 18-cm chamber)

For our standard chamber, the values of k_c and k_t are only 1% different so that for most applications the total exposure rate ($I_c + I_t$) is inferred by simply subtracting the α current from the total current and dividing by the factor corresponding to the dominant component of the radiation field. (In a strict sense, the quantity "exposure rate" is only applied to γ rays of certain energies. However, for environmental radiation fields it is convenient to extend the meaning to include the exposure rate equivalent of ionization in free air due to cosmic rays.) For expressing the exposure rate in SI units, the appropriate quantity would be $C\ kg^{-1}\ s^{-1}$ or $A\ kg^{-1}$. Since this is a rather unfamiliar unit, we prefer to convert the exposure rate to dose rate in air when reporting data in SI units.

A more accurate estimate of I_t is derived by substituting a value for I_c in the above equation. To do this, the altitude of a measurement site is determined using a topographical map or the barometric pressure is measured. The corresponding cosmic-ray exposure rate (dose rate in air) is inferred using the data presented in Figure 3.3. It should be noted that I_c will vary with the 11 year solar cycle, being a few percent higher (lower) at solar minimum (maximum) (O'Brien, 1972).

Although not common with the small freely suspended MOSFET electrometer, stress currents can result from mechanical pressure on the ionization chamber insulator. The presence of these unidirectional currents is checked by reversing the high voltage polarity on the ion chamber shell. After correcting for the electrometer zero offset, the readings

should agree if no stress current is present. If the readings do differ, the true reading is just the arithmetic average of the two.

REFERENCES

Cassidy, M. E., S. Watnick, V. C. Negro, D. C. Freeswick and R. T. Graveson

"A Computer-Compatible Field Monitor System"

IEEE Transactions Nuclear Science, NS-21, 461 (1974)

De Campo, J. A., H. L. Beck and P. D. Raft

"High Pressure Argon Ionization Chamber Systems for Measurements of Environmental Exposure Rates"

USAEC Report HASL-260, December (1972)

Gogolak, C. V.

"Collection and Analysis of Environmental Radiation Data Using a Desktop Computer"

USDOE Report EML-398, April (1982)

Gogolak, C. V. and K. M. Miller

"Method for Determining Radiation Exposure Rates due to a Boiling Water Reactor Plume from Continuous Monitoring Ionization Chambers"

Health Physics, 27, 132-134 (1974)

Latner, N., K. Miller, S. Watnick and R. T. Graveson

"SPICER: A Sensitive Radiation Survey Instrument"

Health Physics, 44, 379-386 (1983)

Negro, V. C., S. Watnick and P. D. Raft

"A Temperature-Compensated Electrometer for Environmental Measurements"

IEEE Transactions Nuclear Science, NS-21, 805 (1974)

O'Brien, K.

"The Cosmic Ray Field at Ground Level"

In: The Natural Radiation Environment II

USERDA CONF-720805-P1, Vol. 1, pp. 15-54 (1972)



Figure 3.1. SPICER system set up for field measurements showing a tripod mounted ion chamber with an electrometer unit connected via cable to the digital readout box.

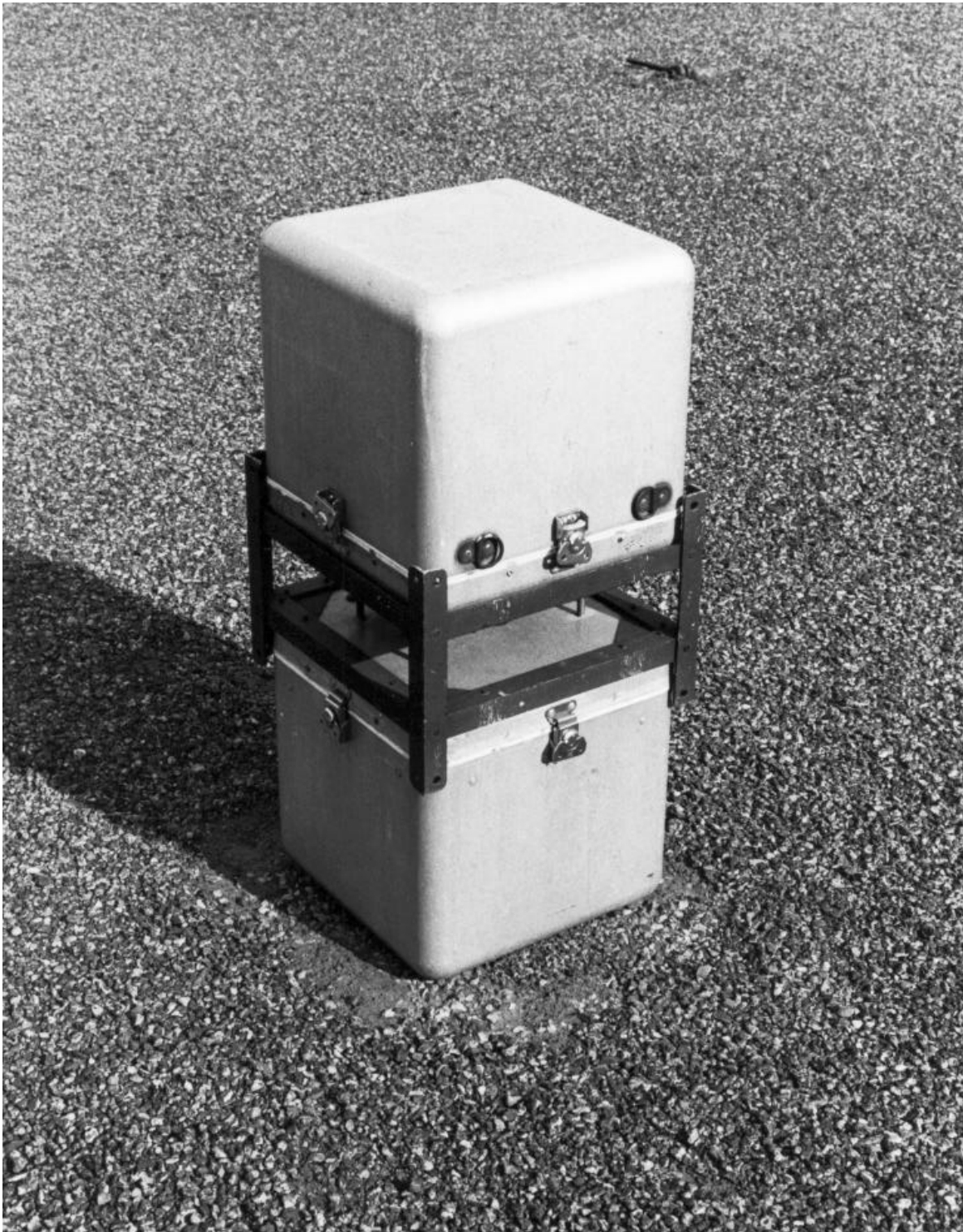


Figure 3.2 PIC system for field monitoring. The chamber and electrometer are housed in the top box, and the digital recorder unit is contained in the bottom box.

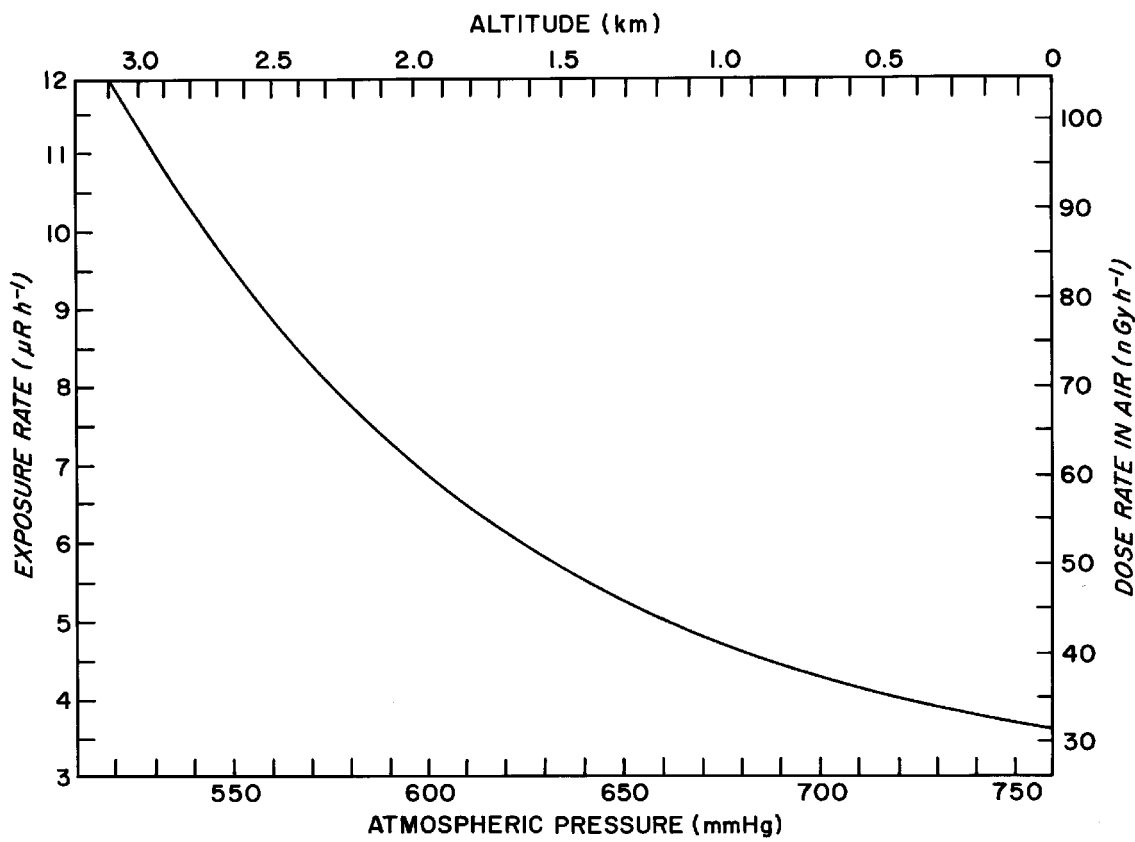


Figure 3.3 Cosmic-ray exposure rate equivalent and dose rate in air as a function of atmospheric pressure and altitude for mid-latitude.

3.3 FIELD GAMMA-RAY SPECTROMETRY

Contact Person(s) : Kevin M. Miller

3.3.1 SCOPE

This section describes the instrumentation, setup, calibration and analysis for EML's field (*in situ*) γ -ray spectrometry using high resolution Ge detectors. The specific application to inventory measurements is described, as well as a spectral stripping routine for total exposure rate measurements. Methods for low resolution NaI detectors are also given.

Field spectrometry is used at EML for the rapid identification of radionuclides in the environment. When the source geometry is taken into account, the concentrations or inventories (activity per unit area) of these radionuclides in the soil can be inferred along with the contribution to the above ground exposure rate. Applications have included:

1. the measurement of natural background and weapons test fallout emitters (Lowder et al., 1964a, b; Beck, 1966; Beck et al., 1964);
2. indoor radiation studies (Miller and Beck, 1984);
3. analysis of power reactor plumes (Gogolak, 1984);
4. the determination of aged fallout levels in terrain with mixed ground cover (Miller and Helfer, 1985).
5. site characterization for environmental restoration (Miller et al., 1994).

3.3.2 INSTRUMENTATION

Although field spectrometry can be performed with a NaI scintillator, the detector of choice at EML for most applications is a high resolution hyperpure germanium coaxial crystal. This type of detector can sustain warmup when not in use, which is a convenient feature during extended field trips.

Ease of handling is best accomplished with a detector mounted in a cryostat that is small (hand-held) and which has an all-attitude capability. Ideally, the detector assembly should be mounted on a tripod with the crystal endcap facing down toward the ground and the dewar above. This orientation maximizes the flux that will be intercepted and registered by the detector. However, a standard 17- or 30-L dewar with an upward facing endcap can still be used without a large loss in efficiency, since most of the flux is incident at the sidewall of the detector, with the dewar blocking out only a few percent of the ground area that is effectively being measured. In either the downward or upward facing geometries, the axis of rotation for the cylindrical crystal is perpendicular to the ground plane. As such, the detector can be assumed to have a symmetrical azimuthal response. A "goose neck" cryostat, where the crystal axis is parallel to the ground plane, should be avoided since this introduces asymmetry and would require making complicated angular corrections.

Counting times in the field can be reduced by using large volume detectors, however, the crystal length/diameter ratio is an important consideration as well. The standard method of measuring the efficiency for a Ge detector is performed with a ^{60}Co source at 25 cm normal to the detector face. As mentioned above, the open field source geometry is such that most of the flux is incident from the side. Thus, for two detectors that have the same quoted efficiency, a long thin crystal will yield a higher count rate in the field as compared to a short wide one. However, length/diameter ratios close to unity would generally result in less uncertainty in measurements due to flatter angular responses.

A list of detectors that we have calibrated for field spectrometry is given in Table 3.1. Our current primary detector for field work is the 45% efficient high purity P-type Ge coaxial mounted in a portable (hand-held) cryostat. It requires a 6 h cool-down time before becoming operational, although it is normally mated to an overhead 30-L liquid nitrogen dewar with a gravity feed system when stored in the laboratory so that it is always ready for use. This type of setup also allows the detector to be placed in a shield

and used for sample analysis. Once cooled down and detached from the feeder dewar, the hand-held cryostat (1.2 L) can be used for as long as 24 h before refilling is required. For studies involving low energy, a recently acquired detector measures 75% in relative efficiency and is of N-type Ge with a beryllium window. It has a 3-L dewar and can be hand-held although it is best suited for tripod mounting.

Generally, measurements are made in the field using a portable battery-powered computer-based spectroscopy system. High voltage and preamplifier power are supplied to the detector by the system. Some detectors feature low power preamplifiers which provide for extended operational time when using battery power in the field. A spectroscopy grade amplifier is also contained within the system. The complete spectrometer system can be carried and operated by one person.

3.3.3 SITE SELECTION AND INSTRUMENT SETUP

The detector is placed ~1 m above the ground with the analyzer and operator positioned a few meters away. The site chosen should be a flat, relatively even and an open area. Terrain that has obstructions such as boulders, large felled or standing trees, and any man-made structures should be avoided as these will block the γ flux from the underlying soil. Extreme ground roughness will result in anomalies since the soil surface area close to the detector is increased, while the surface contribution from large distances is reduced. For measurements of fallout radionuclides, the area must be undisturbed in that water and wind erosion as well as human activity, such as cultivating, would tend to upset the distribution of any deposited activity. Figure 3.4 shows an example of equipment placement at a typical field site.

When selecting a site for measurement, the source geometry must be taken into account. An unshielded detector, placed at 1 m above the ground, samples the photon flux from a volume of soil out to a radius on the order of 10 m and down to a depth of about 30 cm, depending upon the photon energy. Figure 3.5 shows a pictorial representation of the relative ground area contributions to the primary (uncollided) flux at a height of 1 m for a medium energy (662 keV) source with a typical exponential depth profile in the soil. This effective "field of view" varies, being somewhat larger (smaller) for higher (lower) energy sources. Also, activity that is closer to the soil surface will produce a wider field of view. In effect, a field spectrum samples an area of several hundred square meters, thus averag-

ing out the local inhomogeneities in the distribution of the radionuclides. The source being measured is essentially a giant soil sample and counting statistics for a given spectral absorption peak are obtained in a fraction of the time required for counting a small collected sample.

A good practice to follow is to make a series of short measurements in an area to ensure that there is approximate uniformity before collecting a longer spectrum and obtaining the desired counting statistics. When making measurements of natural background, or when the exposure rate is dominated by the man-made emitters under study, this check can be performed with an ionization chamber or a suitably sensitive survey ratemeter in that uniform exposure rate readings would imply a spatially invariant source distribution relative to the detector. If the particular radionuclides under study contribute just a small fraction to the total exposure rate, then the corresponding peak area count rates should be checked with the spectrometer to ensure uniformity.

3.3.4 CALIBRATION

A complete description of field γ -ray spectrometry can be found in Beck et al. (1972) and Miller and Shebell (1995). To summarize, the exposure rate in air above the ground is related to the absorption peak counting rate registered by the detector by

$$\frac{N_f}{I} = \frac{N_0}{\phi} \frac{N_f}{N_0} \frac{\phi}{I} \quad (1)$$

where

N_0/ϕ is the counting rate from a particular spectrum absorption peak due to a unit primary photon flux density of energy E incident on the detector along the detector axis (normal to the detector face).

N_f/N_0 is the correction required to account for detector angular response, and

ϕ/I is the primary photon flux density with an energy E at the detector resulting from the decay of a particular radionuclide per unit exposure rate at the

detector from all primary and scattered photons originating from this nuclide and any others present from its radioactive decay series.

The first two terms depend on the particular detector; ϕ/I values depend only on the source composition and geometry and can be used for any spectrometer calibration.

In a like manner, the concentration or inventory of a particular nuclide is related to absorption peak counting rate by

$$\frac{N_f}{A} = \frac{N_0}{\phi} \frac{N_f}{N_0} \frac{\phi}{A} \quad (2)$$

where ϕ/A is the total photon flux density at the detector location per unit concentration or inventory of the nuclide.

The three factors to compute N_f/I or N_f/A are discussed separately.

A. N_0/ϕ .

The response to unit flux at normal incidence is evaluated for a detector using various γ -ray point sources. A complete energy response curve from 40 keV to 3 MeV can be inferred with a set made up with the reasonably long lived isotopes ^{152}Eu , ^{241}Am , ^{137}Cs , ^{60}Co , and ^{228}Th . The measurement procedure is as follows:

1. Position the source at a distance of at least 1 m and at normal incidence to the detector face.
2. Calculate the uncollided flux density at the detector effective crystal center, which is obtained by dividing the γ emission rate by $4\pi r^2$. The value of r is the distance from the source to the crystal effective center. This can be taken to be the geometric center for high energy (> 1 MeV) rays and the crystal face for low energy (< 0.1 MeV) γ rays. For the energy range between these two values, an estimate of average penetration distance can be made based on the absorption coefficient of the crystal. The γ flux density is also corrected for air and source holder attenuation.
3. Collect a spectrum and determine the full absorption peak count rate.

4. Collect a spectrum without the source present and subtract out from the previously measured count rate any contribution to the peak from background emitters.
5. Divide the corrected count rate by the flux density to determine N_o/ϕ .
6. Perform this measurement at different energies with either simultaneous or separate runs.
7. Plot the values of N_o/ϕ versus energy on a log-log scale and fit the data to a smooth curve. Figure 3.6 shows N_o/ϕ as function of energy above 200 keV for the detectors listed in Table 3.1. In the energy range shown, the response can be fit to a straight line on a log-log plot to within $\pm 3\%$.

B. N_f/N_o .

The uncollided γ -ray flux for a soil half space source geometry is not limited to angles normal to the detector face. Therefore, the complete flux density response calibration must account for the fact that a cylindrical Ge crystal when oriented with the axis of symmetry perpendicular to the ground plane has a variable altitudinal (zenith-angle) response. The correction factor, N_f/N_o , is determined from point source calibrations as functions of energy and angle in the vertical plane and can be calculated from

$$\frac{N_f}{N_o} = \int_0^{\frac{\pi}{2}} \frac{\phi(\theta)}{\phi} \frac{N(\theta)}{N_o} d\theta \quad (3)$$

where

$\phi(\theta)/\phi$ is the fraction of the total primary flux at zenith angle θ for a given source energy and geometry, and

$N(\theta)/N_o$ is the response of the detector at angle θ for the same energy γ ray relative to the response at normal incidence.

The procedure for determining the values of N_f/N_o is as follows:

1. Measure the full absorption peak count rate (minus any background contribution to the peak) using a point source at a fixed distance of at least 1 m to the crystal at 15° intervals between incident angles of 0° (normal to detector face) and 90°.
2. Plot the relative response $N(\theta)/N$ versus angle and fit the data to a smooth curve.
3. Evaluate Equation 3 numerically for at least three different source distributions in the soil (surface plane, 3 cm relaxation depth, and uniform). The angular flux distribution data can be found in Beck et al. (1972).
4. Repeat Steps 1-3 for several other energies and plot the resultant values of N_f/N_o versus energy. The data points can be fit to a smooth curve for each source depth distribution.

As noted before, a longer crystal would tend to yield a higher count rate in the field, meaning that the value of N_f/N_o would be > 1 . For the source distributions generally encountered, more than 80% of the uncollided flux is incident between $\theta = 30^\circ$ - 90° (θ measured from the detector axis normal to the ground interface). Uniformity of the zenith angular response in this range to within a few percent assures that the value of N_f/N_o will not vary significantly with changes in the distribution of flux. In general, a more uniform response is achieved with a crystal where the diameter is close to the length dimension. However, the variation in N_f/N_o for a detector where the crystal length/diameter is as high as 1.3 or as low as 0.7 would not be expected to be more than about 20% for energies > 200 keV. Figure 3.7 shows angular correction factor data at three different energies for several detectors in a downward facing geometry and a uniform source depth profile.

C. ϕ/I and ϕ/A .

The ϕ/I (and ϕ/A) factors are derived from γ -ray transport calculations. Tabulations of these data along with other pertinent information on the make-up of the environmental γ radiation field can be found in Beck et al. (1972), Beck and de Planque (1968), and Beck (1972). A complete set of exposure rate values (I/A) for close to 200 common fission and activation isotopes at various exponential depth distributions in the soil can be found in Beck (1980).

Notes:

1. The inference of exposure rates from nuclides located in the ground does not require a precise knowledge of the distribution with depth or of the exact soil density or composition. This property results because the observed peak count rate in a field spectrum is essentially a measure of the uncollided flux, and although this quantity and the exposure rate produced by it and the associated scattered flux varies significantly with the source depth distribution and soil characteristics, the ratio of these two quantities, ϕ/I , does not. Thus, even a crude estimate of source distribution should not lead to a sizeable error in the exposure rate.
2. In lieu of a complete experimental calibration of a Ge detector for field spectrometry, generic factors may be substituted at energies > 200 keV (Helfer and Miller, 1988). The only parameters needed to apply this semiempirical calibration method are the manufacturer's quoted efficiency at 1332 keV (5-45%), the crystal length/diameter ratio (0.5-1.3), and the detector orientation in the field (upward or downward facing). The accuracy of the derived factors is estimated to be $\pm 10\%$ for energies > 500 keV and $\pm 15\%$ for energies between 200 and 500 keV.

3.3.5 SPECTRUM ANALYSIS

In many situations, the built-in peak area estimate features of state-of-the-art analyzers are used in providing quick results in the field. Prominent peaks are identified in a benchmark spectrum and the appropriate regions of interest are set up. On certain analyzers, function keys are programmed using the net peak area, counting time and calibration factor (N_p/I and N_p/A) to provide instantaneous readout of exposure rate and concentration or inventory.

For more complete data reduction, a small computer is interfaced to the analyzer to run a spectrum analysis program. If desired, a totally portable system may be configured using a battery-powered laptop computer. Our standard analysis program (Gogolak and Miller, 1977; Gogolak, 1982) performs the following:

1. Based on a two point energy calibration as set by the operator, certain peaks which are characteristic of typical environmental spectra are identified, namely:

- a. the 186, 295, 352, 609, 1120 and 1765 keV peaks in the ^{238}U series;
- b. the 583, 911, 966 and 2615 keV peaks in the ^{232}Th series;
- c. the 1460 keV peak of ^{40}K ;
- d. the 662 keV peak of ^{137}Cs .

These peaks are defined by set energy bands where the left and right channel markers are representative of the Compton continuum.

2. The counts between the energy boundaries for each of the above peaks are summed. The background counts in three channels on each side of a peak are averaged and the result is used as an estimate of the baseline under the peak. This is multiplied by the number of channels in the peak and subtracted out from the total counts in the peak band to yield the net peak counts.
3. Detector specific calibration factors are applied to convert from peak count rate to exposure rate and concentration or inventory.
4. A printout is made listing count rates, converted quantities and associated statistical counting errors.
5. Permanent storage of the spectrum is made on either magnetic tape or diskette.
6. As an option, an automated search is performed to identify any peaks present in the spectrum. Data such as nuclide, half-life, γ -ray intensity and associated energy are printed out using a library of nearly 400 principal γ -ray energies that are seen in the environment (Section 5, this Manual). Any peak can be quickly analyzed by using an optional automated continuum strip.
7. The program enters an interactive phase where the operator examines any additional peaks, checks the results of the automated routine, or investigates any unusual or unexpected features of a spectrum.

3.3.6 INVENTORY MEASUREMENTS

3.3.6.1

APPLICATION

A field γ -ray spectrum can also provide an estimate of the amount of activity per unit area of soil surface for nuclides which have been deposited on the ground. To do this, a knowledge of the source distribution in the soil is required in order to relate the measured total absorption peak count rate to the incident unscattered photon flux and then to the activity in the soil in a manner analogous to that used for natural emitters.

The activity profile with depth for deposited nuclides in undisturbed soils can be represented by an exponential function,

$$S = S_0 e^{-(\lambda/\rho) z} \quad (4)$$

where

- S is the activity per cm^3 at depth z cm,
- S_0 is the activity per cm^3 at the soil surface,
- λ is the reciprocal of the relaxation length in cm^{-1} , and
- ρ is the *in situ* soil density (g cm^{-2}).

The cumulative activity, or inventory I , integrated to depth z' is, then,

$$I = \int_0^{z'} dz = \frac{S_0}{\lambda} [1 - e^{-(\lambda/\rho) z'}] = I_0 [1 - e^{-(\lambda/\rho) z'}] \quad (5)$$

where I_0 is the total inventory integrated to infinite depth.

3.3.6.2

HOMOGENEOUS TERRAIN

In the case of a freshly deposited nuclide, the depth parameter is infinite corresponding to a plane source distribution and a relaxation length of zero. In practice, the effects of ground roughness bury the source somewhat. Even on what appears to be flat terrain, we apply an λ value of $6.25 \text{ cm}^2 \text{ g}^{-1}$, which at a typical soil density of 1.6 g cm^{-3} corresponds to a relaxation depth of 0.1 cm. Values of λ for aged global fallout ^{137}Cs have been found to range from a high of 1.0 for an evergreen forest floor to a low of 0.03 for a flood irrigated lawn. At a soil density of 1.6 g cm^{-3} , these correspond to relaxation lengths of 0.6 and 21 cm, respectively. More typical values of λ tend to range from 0.05-0.1 for open field sites and 0.2-0.5 for wooded or desert areas.

Values of the unscattered flux and its angular distribution at 1 m above the ground have been tabulated for exponentially distributed sources in the soil for various energies and λ values (Beck et al., 1972). Using Equation 2, where the term A now represents the inventory (activity per unit area), the detector response can be calculated for a particular nuclide as a function of λ . If the nuclide has two reasonably strong γ lines well separated in energy, the value of λ can be inferred from the ratio of the measured fluxes.

In the case of a monoenergetic source such as ^{137}Cs , the value of λ can be determined experimentally as follows:

1. A 62 cm^2 or similar large area corer and auger is used to extract soil samples from different depth intervals (see Section 2.4) depending upon the expected activity distribution. For example, if the profile is expected to be shallow, the depth intervals can be 0-2.5, 2.5-5, and 5-30 cm, while if it is expected to be deep, intervals of 0-5 cm, 5-10 cm, and 10-30 cm can be used. More than one core can be taken, in which case the samples from the same depth are composited. The depth of the soil core should be sufficient to include essentially all of the deposited activity so that I_0 can be determined.
2. An aliquot of a sample from each depth increment is counted on a high resolution Ge detector to determine the concentration of the radionuclide of interest.

3. The activity per unit area for each depth is computed from the product of the concentration and the sample mass for that depth increment divided by the area of the sample.
4. A fit to Equation 5 is then applied, the variables being $I_0 - I$, the integrated activity per unit area and z' , the gross *in situ* mass per unit area down to depth z' . Graphically, this can be performed by plotting the $\log(I_0 - I)$ versus z and fitting a straight line through the points, weighting the points near the surface more heavily since this is where most of the activity is contained. The slope of this line is just $1/z$.

Note:

Although the inventory is determined using the soil sample data itself, it is quite useful to corroborate this estimate with the field spectrum. The soil cores may represent an area of a few hundred square centimeters, while the field data represent the average over several hundred square meters.

3.3.6.3

NONHOMOGENEOUS TERRAIN

For areas where the fallout is suspected of being unevenly distributed across the ground, representative inventory measurements can still be made by relying on the fact that a field spectrum averages out the local inhomogeneities in the source geometry. This more generalized method is applied to cases such as the measurement of aged fallout in the desert southwest of the U.S. where blowsand tends to shift from bare soil and collect under vegetative cover. A complete description can be found in Miller and Helfer (1985). The basic steps include:

1. Soil samples in depth increments are collected from the different types of ground cover present (grass, brush, bare soil, etc.).
2. The samples are counted and a depth profile for each type of ground cover is obtained using the procedure outlined above for homogeneous terrain.

3. If the depth profiles are significantly different, the approximate percentage of ground cover of each type is determined within a 15 x 15 m square centered at the detector. This can be performed using a combination of tape measurements and eye estimates to approximate the dimensions of any patches of grass or shrubs and trees out to their drip line, or to where there is an obvious change in soil characteristics, and then calculating the total area of each particular type of cover.
4. The conversion factor to apply to the peak count rate in order to obtain an inventory estimate is given by

$$\langle g \rangle = \left[\sum_i \frac{x_i}{g_i} \right]^{-1} \quad (6)$$

where

- $\langle g \rangle$ is the average full absorption peak count rate to inventory conversion factor for an infinite half space source distribution with randomly spaced segments of different types of ground cover, each of which has its own characteristic nuclide depth distribution and inventory (inventory per unit count rate),
- x_i is the fraction of the total inventory associated with the i-th type of ground cover,
- g_i is the full absorption peak count rate to inventory conversion factor for an infinite half-space source distribution with a measured depth profile characteristic of the i-th type of ground cover (inventory per unit count rate).

Note:

The value of $\langle g \rangle$ exhibits a dependence on the relative inventory mix for the different ground covers which can only be determined through soil sampling. Nonetheless, the value of $\langle g \rangle$ must fall within the range of the individual values of g_i . Generally, this range is not large. Although the inventory may typically vary by a factor of two for the different ground covers, the variation in the conversion factor for the different depth profiles associated with these ground covers will average <30%. This is particularly true for sites where the fallout is near the soil surface because the conversion factor does not vary strongly with the depth profile for values of $h/z > 0.2$.

3.3.7 SPECTRAL STRIPPING FOR GERMANIUM DETECTORS

3.3.7.1

APPLICATION

A stripping operation can be applied to a Ge detector spectrum which has been collected in free air in order to obtain the γ flux density as a function of energy (Miller, 1984). This flux spectrum can be readily converted to an independent estimate of the free air exposure rate or be used to make energy response corrections to other radiation measuring devices. This technique has particular applications to indoor radiation measurements, where the flux distribution is not easily predicted because of the complex and generally unknown γ source geometry.

3.3.7.2

THEORY

A count registered by the detector can be caused by the full or partial absorption of an incident photon or by the passage of a cosmic ray produced charged particle. In order to obtain a measure of the incident photon flux spectrum, the partial absorption and cosmic-ray events must be subtracted out and then the full absorption efficiency curve of the detector can be applied.

The stripping operation can be expressed as:

$$N_i' = N_i - \sum_{j=i+1}^L f_{ij}(r_j - 1)N_j' - N_c \quad (7)$$

where

N_i', N_j' are the counts in an energy band due to the total absorption of incident γ flux,
 N_i is the observed counts in an energy band due to all sources,
 L is the energy band containing the highest energy γ line (generally 2.615 keV),

- f_{ij} is the fraction of the continuum counts at energy band i due to the partial absorption of incident γ flux at energy band j ,
 r_j is the ratio of total counts to full absorption peak counts for incident flux at energy band j , and
 N_c is the counts in band i due to cosmic-ray events, assumed to be constant in any energy band and given by

$$N_C = (E_2 - E_1 + 1)^{-1} \sum_{i=E_1}^{E_2} N_i \quad (8)$$

where

E_1, E_2 are the lower and upper energy bands of a pure cosmic-ray energy (generally 3-4 MeV).

3.3.7.3

DETERMINATION OF STRIPPING PARAMETERS (f and r)

Factor f - For the factor f , a multiple step function fit is used wherein the region below the Compton edge is divided into 10 equal size energy bands and the region above the Compton edge is divided into four equal bands. The fraction of the total counts in the continuum in each band can be experimentally determined for a particular detector by examining the shape of the continuum below a full absorption peak from a monoenergetic γ source. Although the shape of the continuum is a function of the energy and incident angle of the γ ray, it is not overly sensitive to these variables, particularly at the higher energies which contribute the most to the exposure rate.

Factor r - In the same manner that the full absorption peak efficiency is determined for a detector (see Procedure 3.3.4 for N_o/ϕ), the total efficiency can be determined and its ratio computed. However, effectively monoenergetic sources must be used and room background must be subtracted from the entire spectrum. Like the full absorption peak efficiency, the total efficiency varies with incident angle for a cylindrical detector. However, the ratio of the two, r , varies more smoothly and is not a strong function of the incident angle. A single angular correction factor can therefore be applied which is representative of the higher γ energies which weigh heavily in the exposure rate computa-

tion. This factor can be obtained by assuming an isotropic radiation field and averaging over the entire 4π solid angle. Although, in practice, the radiation field may not be isotropic, a reasonable approximation to this ideal can be created by accumulating a spectrum with the detector oriented in different directions, thus averaging out the angular dependence. To accomplish this, we routinely count for equal lengths of time with the detector pointing in six different directions, that is, each way along three orthogonal axes.

3.3.7.4

STRIPPING OPERATION

The stripping operation is performed on a portable PC using Basic and takes < 1 min to complete. It proceeds as follows:

1. The spectrum is calibrated using two energy-channel points supplied by the operator.
2. The spectrum is compressed from 4000 channels to 400 channels for faster computation.
3. The spectrum is stripped of the cosmic-ray events.
4. The spectrum is stripped of partial absorption events for equal size energy bands of 10 keV each and starting at the band containing the highest energy γ line (generally 2.615 keV), where $N' = N - N_c$. Succeeding lower energy bands can then be computed based on the N'_j values from any higher band.
5. The spectrum of counts which remains after the stripping operation is completed is converted to the incident flux density energy distribution by applying the full absorption peak efficiency of the detector. As in the case of the factor r , an angular correction based on the assumption of isotropic incidence must be applied.
6. The γ exposure rate is computed by integrating across the spectrum the product of the energy, flux density, and mass energy absorption coefficient for air at each energy band.

Note:

Intercomparisons between the spectral stripping method and our own instruments and standard procedures, as well as with those of the Japanese Atomic Energy Research Institute, have shown good agreement (Nagaoka, 1987). Based on these measurements, we conservatively estimate an upper limit in the total systematic error of $\pm 5\%$ when this method is applied to spectra at background levels. The statistical error was determined to be $< \pm 2\%$ (at the 1 σ level) for a 1-min spectrum at typical background levels.

3.3.8 SODIUM IODIDE DETECTORS

3.3.8.1

APPLICATION

Although no longer used routinely by EML for field γ -ray spectrometry, NaI detectors are nonetheless capable of yielding satisfactory results particularly for natural background measurements. Like the case for Ge detector measurements, full absorption analysis can be applied to a NaI field spectrum. In addition, there is the technique of "energy band" analysis as well as "total spectrum energy" analysis. A complete description of these methods can be found in Beck et al. (1972).

3.3.8.2

EQUIPMENT

The NaI detectors (usually 4-x-4 in cylindrical crystals attached to matched photomultiplier tubes) are coupled through an emitter-follower preamplifier. Either a battery powered portable or 120 V AC vehicle-based analyzer with at least 400 channels is used to collect the spectra. NaI detectors are usually covered (in addition to the manufacturer's standard thin aluminum or stainless steel window) by a 6-mm bakelite shield to reduce the β -ray contribution to the Compton continuum as well as to moderate thermal stresses. The NaI detector is transported in a rugged, foam-cushioned box to minimize mechanical and thermal shock.

3.3.8.3

PEAK ANALYSIS

For NaI spectrometry, the N_o/ϕ should be obtained with source energies as close as possible to those environmental sources to be evaluated, usually the energies associated with the ^{238}U and ^{232}Th series, ^{40}K , and ^{137}Cs . The resulting N_o/ϕ versus E data do not represent the usual NaI response curve, because the analysis of absorption peaks does not lead to accurate estimates of the actual peak areas, unless one engages in a complex computer program for spectral stripping. NaI peak areas are determined in essentially the same manner as those from Ge detectors, though only a few absorption peaks are measurable due to the relatively poor resolution. Cross-calibration of a NaI detector with the more accurate Ge detector can be very helpful.

3.3.8.4

ENERGY BAND ANALYSIS

When the naturally-occurring nuclides associated with the ^{238}U and ^{232}Th series and ^{40}K predominate at a field site, the simplified "energy band" method of analysis can be applied. In this method, the spectrum energy is calculated as the product of the counts per channel times the energy represented by each channel in bands of channels. The energy bands are centered on the 1.46 MeV ^{40}K , the 1.76 MeV ^{214}Bi , and the 2.62 MeV ^{208}Tl peaks. The response in each bin can then be represented by the following equations.

$$E_1 = u_1U + k_1K + t_1T + I_1$$

$$E_2 = u_2U + k_2K + t_2T + I_2 \quad (9)$$

$$E_3 = t_3T + I_3$$

where E_1 , E_2 and E_3 are the measured "energy" values for some arbitrary counting period;

U, K and T represent the exposure rates to be measured; the constants represent the distribution of spectrum energy per unit exposure rate among the three energy bands; and I_1 , I_2 and I_3 are the cosmic-ray contributions. The three equations relating the U, K and Th exposure rates to the energy bands are determined by solving Equation 9 and evaluating the coefficients from regression analyses of a large number of field spectra for which exposure rates had been determined from absorption peak analyses.

The following approximate equations apply for a nominal 10.16 x 10.16 cm NaI detector, shielded with 6-mm Bakelite, though calibration of individual detectors is preferred.

$$U = 0.4 E_1' - 0.2 E_3'$$

$$K = 0.08 E_1' - 0.06 E_2' - 0.02 E_3' \quad (10)$$

$$T = 0.3 E_3'$$

and

$$I = E_T'/37$$

where I is the total exposure rate from natural radioactivity in soil, and

$$1.32 \text{ MeV} < E_1' < 1.60 \text{ MeV},$$

$$1.62 \text{ MeV} < E_2' < 1.90 \text{ MeV},$$

$$2.48 \text{ MeV} < E_3' < 2.75 \text{ MeV},$$

$$0.15 \text{ MeV} < E_T' < 3.40 \text{ MeV},$$

the E values being in GeV per 20-min counting period. The primes indicate that the energy contributions from cosmic rays must be subtracted before Equations 10 are used.

Energy band analysis is performed quickly in the field by interfacing the multichannel analyzer to a portable computer. Using interactive software (Gogolak and Miller, 1977), the basic steps include:

1. The spectrum is read into the computer and the operator provides a two point energy calibration (usually the positions of the 1460 keV ^{40}K and 2615 keV ^{208}Tl peaks) and the altitude to the nearest thousand feet (for the cosmic-ray corrections).
2. The above equations are applied.
3. A printout is made of the total exposure rate and the contributions for ^{40}K and the ^{238}U and ^{232}Th series.

3.3.8.5

TOTAL SPECTRUM ENERGY ANALYSIS

The exposure rate in air is proportional to $\int_0^\infty \phi(E) (\mu_{\text{e}}/) \text{E} d\text{E}$, where $\phi(E)$ is the flux of γ rays of energy E and $\mu_{\text{e}}/$ is the mass absorption coefficient in air. Between a few hundred keV and several MeV, $\mu_{\text{e}}/$ is fairly constant. Also for low energies, the probability of an incident photon being totally absorbed by a large NaI detector is fairly high (on the order of 50-100% from 100 keV to 1 MeV). About 75% of the exposure rate from the soil is due to emitters between 100 keV and 1500 keV. This and the fact that the spectrum of γ rays from natural emitters is fairly invariant to the exact proportions of U, Th and K in the soil, indicates that the total "spectrum energy" is a reasonable measure of free air exposure from natural radioactivity in the soil. A large NaI or similar detector measures the flux to a fairly high degree of accuracy and, even though sensitivity decreases somewhat at higher energies due to the escape of secondary scattered photons, this decrease tends to be compensated by correspondingly smaller values of $\mu_{\text{e}}/$ for energies above 1 MeV relative to values below 1 MeV.

Unlike many NaI hand-held survey instruments, which depend on the assumption that the counting rate above some bias level is proportional to the exposure rate, the total energy technique requires only that the counts in a channel be proportional to $\phi(E) (\mu_{\text{e}}/)$ for that energy, and is, therefore, less sensitive to spectral changes. For example, a NaI survey meter might indicate that the exposure rate from a unit flux of 60 keV photons as being almost equal to the exposure rate from a unit flux of 1460 keV photons. This would occur since the 1460 keV pulse would be recorded due to the high probability of a Compton collision in the detector even though many of the secondaries would escape the crystal. In the total energy technique, the higher energy counts are weighted by the energy

deposited and reflect their relative contribution to the exposure rate more correctly. The slightly larger total absorption at 60 keV reflects the larger value of $(\mu_e/)$ relative to higher energy γ rays.

The spectrum "energy" calibration factors for 10.16 x 10.16 cm detectors are determined in two ways:

1. The detectors are exposed to a known point source of ^{226}Ra in the laboratory and the measured exposure rate is compared to an ionization chamber reading. The measurement should be corrected to account for the fact that the rays from the point source are incident along the detector axis.
2. A comparison of measurements of "spectrum energy" from actual field spectra is made with simultaneous ionization chamber measurements for different environmental radiation fields.

The two methods give essentially the same calibration factors.

REFERENCES

Beck, H. L.

"Environmental Gamma Radiation from Deposited Fission Products, 1960 - 1964"
Health Physics, 12, 313-322 (1966)

Beck, H. L.

"The Physics of Environmental Gamma Radiation Fields"

J. A. S. Adams, W. M. Lowder, and T. F. Gesell (Editors)

In: *The Natural Radiation Environment II*, CONF-720805-P1, pp. 101-134 (1972)

Beck, H. L.

"Exposure Rate Conversion Factors for Radionuclides Deposited on the Ground"

USDOE Report EML-378, July (1980)

Beck, H. L. and G. de Planque

"The Radiation Field in Air Due to Distributed Gamma-Ray Sources in the Ground"

USAEC Report HASL-195, May (1968)

Beck, H. L., W. J. Condo and W. M. Lowder

"Spectrometric Techniques for Measuring Environmental Gamma Radiation"

USAEC Report HASL-150, October (1964)

Beck, H. L., J. A. De Campo and C. V. Gogolak

"In Situ Ge(Li) and NaI(Tl) Gamma-Ray Spectrometry for the Measurement of
Environmental Radiation"

USAEC Report HASL-258, July (1972)

Gogolak, C. V.

"Collection and Analysis of Environmental Radiation Data Using a Portable Desktop
Computer"

USDOE Report EML-398, April (1982)

Gogolak, C. V.

"Rapid Determinations of Noble Gas Radionuclide Concentrations in Power Reactor
Plumes"

Health Physics, 46, 783-792 (1984)

Gogolak, C. V. and K. M. Miller

"New Developments in Field Gamma-Ray Spectrometry"

USDOE Report EML-332, December (1977)

Helfer, I. K. and K. M. Miller

"Calibration Factors for Germanium Detectors Used for Field Spectrometry"

Health Physics, 55, 15-29 (1988)

Lowder W. M., H. L. Beck, and W. J. Condo

"Spectrometric Determination of Dose Rates from Natural and Fall-Out
Gamma-Radiation in the United States, 1962-63"

Nature, 202, 745 (1964a)

Lowder W. M., W. J. Condo and H. L. Beck

"Field Spectrometric Investigations of Environmental Radiation in the U.S.A."

In: *The Natural Radiation Environment*, University of Chicago Press, Chicago, IL,
pp. 597-616 (1964b)

Miller, K. M.

"A Spectral Stripping Method for a Ge Spectrometer Used for Indoor Gamma
Exposure Rate Measurements"

USDOE Report EML-419, July (1984)

Miller, K. M. and H. L. Beck

"Indoor Gamma and Cosmic Ray Exposure Measurements Using a Ge Spectrometer
and Pressurized Ionisation Chamber"

Radiation Protection Dosimetry, 7, 185-189 (1984)

Miller, K. M. and I. K. Helfer

"*In Situ* Measurements of ^{137}Cs Inventory in Natural Terrain"

In: Environmental Radiation '85, Proceedings of the Eighteenth Midyear Topical
Symposium of the Health Physics Society, pp. 243-251 (1985)

Miller, K. M. and P. Shebell

"*In Situ* Gamma-Ray Spectrometry - A Tutorial for Environmental Radiation Scientists"

USDOE Report EML-557, October (1995)

Miller, K. M., P. Shebell and G. A. Klemic

"*In Situ* Gamma-Ray Spectrometry for the Measurement of Uranium in Surface Soils"

Health Physics, 67, 140-150 (1994)

Nagaoka, T.

"Intercomparison Between EML Method and JAERI Method for the Measurement of
Environmental Gamma Ray Exposure Rates"

Radiation Protection Dosimetry, 18, 81-88 (1987)

Table 3.1
Ge DETECTOR SPECIFICATIONS

Manufacturer	Serial No.	Code	Type	Cryostat orientation	Efficiency (%)	Resolution at 1332 (keV)	Dimensions DxL (mm)	L/D ⁺	Peak/Compton
*Princeton Gamma-tech	484	P1	Ge(Li)	4 L, downward	2.9	1.70	36 x 20	0.56	23.0
	514	P2	Ge(Li)	4 L, downward	12.2	2.43	43 x 44	1.02	30.0
	1039	P3	Ge(Li)	17 L, upward	27.9	2.36	59 x 47	0.80	35.9
	1545	P4	Ge(Li)	17 L, upward	22.3	2.10	56 x 54	0.96	49.5
	1030	P5	P-type Ge	2 L, all attitude	21.7	1.77	59 x 35	0.59	52.0
**EG & G Ortec	23-N-37VB	O1	N-type Ge	30 L, upward	35.3	1.96	55 x 65	1.18	59.4
	25-N-1514	O2	N-type Ge	30 L, upward	35.4	1.73	55 x 73	1.31	67.9
	26-P-70P	O3	P-type Ge	1.8 L, all attitude	45.0	1.80	60 x 79	1.31	73.0
	33-TN30860A	-	N-type Ge	3 L, all-attitude	75.0	1.95	71 x 79	1.11	74.8

*Princeton Gamma-Tech, Inc., 1200 State Road, Princeton, NJ 08540

**EG & G Ortec, 100 Midland Road, Oak Ridge, TN 37830

⁺Ge crystal length/diameter ratio



Figure 3.4. Typical field site for conducting *in situ* γ -ray spectrometry showing placement of tripod mounted portable Ge detector and battery-powered multichannel analyzer.

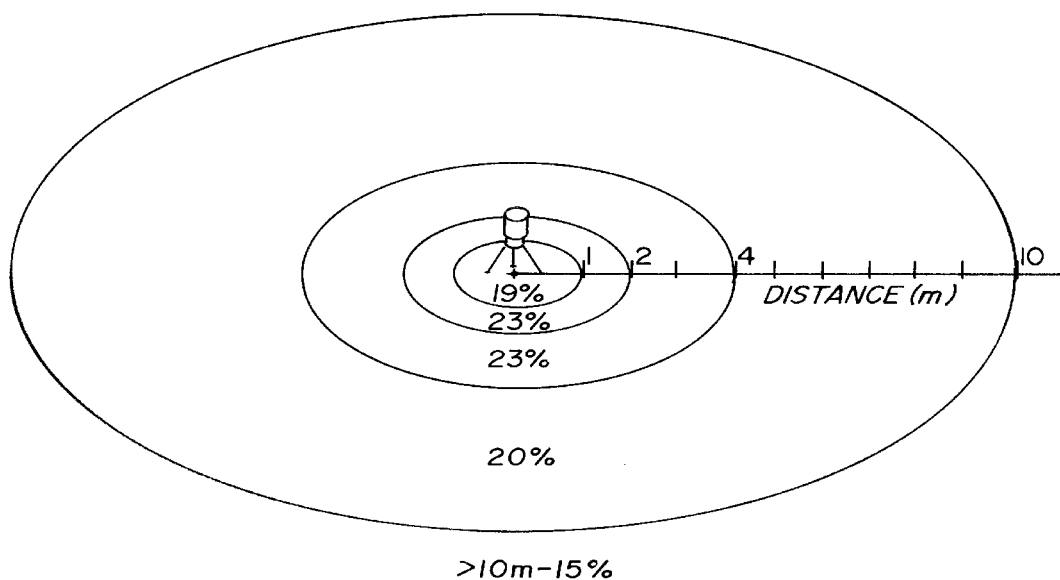


Figure 3.5. Schematic representation of the relative ground area contributions to the primary flux at 1 m above the ground for an exponentially distributed source with an energy of 662 keV and where $\lambda = 0.21 \text{ cm}^2 \text{ g}^{-1}$.

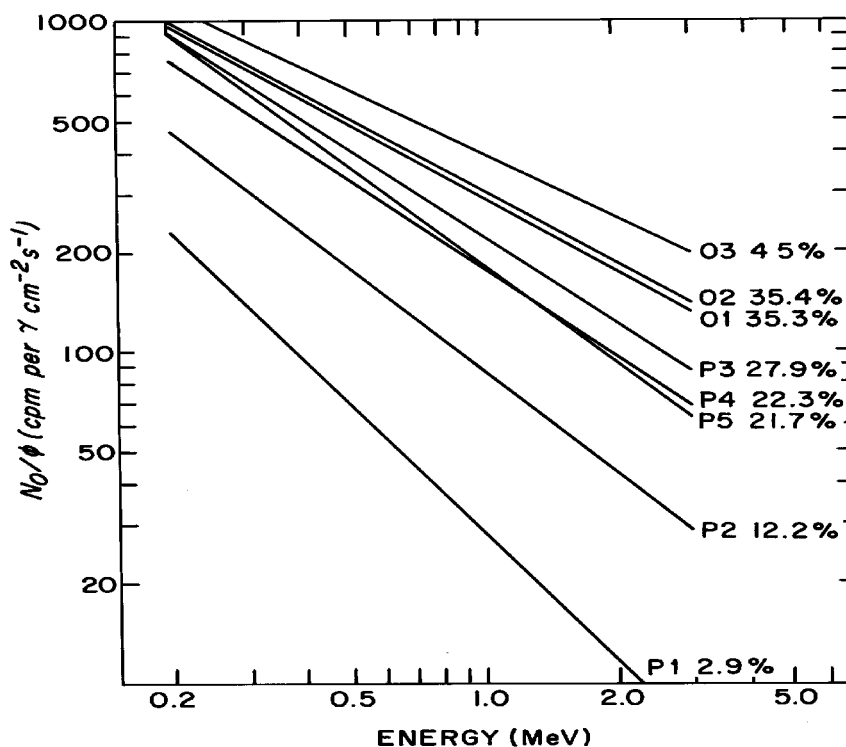


Figure 3.6. Count rate per unit incident flux at normal incidence (N_0/ϕ) as a function of energy for seven of the detectors listed in Table 3.1.

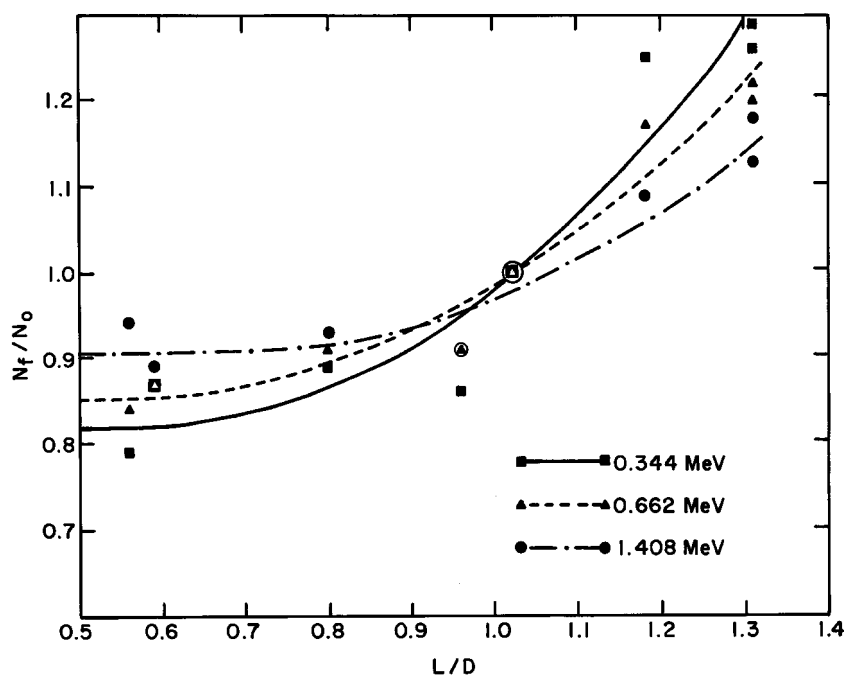


Figure 3.7. Angular correction factor (N_f/N_0) as a function of Ge crystal length/diameter (L/D) ratio at three different energies for a downward facing detector for a uniform with depth source profile in the soil.

3.4 REMOTE GAMMA-RAY SPECTROMETRY STATIONS

Contact Person(s) : Colin G. Sanderson

3.4.1 SCOPE

EML's global studies are comprised of a Global Fallout Program, a Surface Air Sampling Program, and a Remote Atmospheric Measurements Program (Sanderson et al., 1994). These programs currently represent EML's effort to sample, measure, and study radionuclides in the lower troposphere and their deposition on the earth's surface (Larsen et al., 1994).

Using remote atmospheric measurement systems (RAMS) in RAMP, EML is able to measure gamma-ray emitting radionuclides having short half-lives, such as ^7Be , that have been collected by drawing air through highly efficient filters, see Procedure 2.2.2.2. The gamma-ray spectrum is transmitted to ARGOS communications systems flown aboard polar-orbiting National Oceanic and Atmospheric Administration (NOAA) satellites, retransmitted to ground stations, and recovered via a telephone link by EML's computer. The recovered sodium iodide (NaI) gamma-ray spectrum is automatically resolved using a linear least squares program with a library of 18 possible gamma-ray emitting radionuclides. The last background spectrum received is also included in the library. When the analysis is complete, the results are written to a report file and a computer mail message is issued to report the completion of the analysis.

Once a RAMS station has been set up, its weekly operation requires <1 h of an operator's time. Each week one sample, one calibration, and one background is counted. Each month the weekly air filter samples are sent to the University of Miami and the computer floppy disk is sent to EML.

3.4.2 COMPONENTS

A. Gamma-ray detector.

A 12.7 cm x 10.2 cm diameter integral inline NaI(Tl) gamma-ray detector with ^{241}Am doping for gain stabilization is used in the RAMS. The photopeak produced by the ^{241}Am alpha particles should approximate a 3.5 MeV gamma ray.

B. Lead shield.

The copper-lined shield is composed of 12 interlocking steel and lead rings with a sample holder drawer at its base. The rings are 27 cm in diameter at the lower half and 22 cm for the top half of the shield and weigh either 20 kg or 9 kg, depending on the size.

C. Heated environmental chamber.

A heated environmental chamber is used to house the lead shield, NaI detector, multiplying phototube, and preamplifier. The temperature inside the chamber is set ~ 5°C above the highest expected ambient temperature.

D. Lead-acid gel-cell batteries and DC charger (power supply system).

The power supply system provides primary and backup battery power to the RAMS. This system uses: a transformer to convert 240-V power to 120 V (if required); sealed, lead-acid gel-cell batteries; and battery chargers. The EML-designed power supply can sustain 8 h of continuous operation when a line power failure occurs.

E. Multichannel analyzer (MCA).

The portable MCA used in the RAMS has the following features: 4096 channel, battery operated, CRT display, preamplifier power, detector high voltage, RS232 input/output. Davidson Model #2056-C MCA or equivalent is used.

F. Laptop computer.

A computer with backlite LCD display, either dual floppy, one fixed and one floppy disk, at least one RS232 and one parallel port, 512K memory, and simple 12-V DC operation are required.

G. Satellite transmitter and antenna.

A 2 W, 401.650 MHz transmitter, 30.5 m of low-loss cable and an omnidirectional quadrafilar helix antenna are used to transmit the gamma-ray data to the ARGOS satellites. Polar Research SITRA-1 or SITRA-2 or equivalent is used.

Figure 3.8 shows a block diagram of EML's second generation NaI RAMS.

3.4.3 INSTRUMENTATION ASSEMBLY

A. Lead shield and NaI detector.

Place the removable bottom of the environmental chamber on a table or floor that will support about 200 kg. The shield parts are numbered for assembly. Place the lead base (1) on the indicated circle. Place lead ring (2) on top of (1) and lead ring (3) on top of (2). Align these rings so that the sample drawer fits properly. Continue to install lead rings (4), (5), and (6). Next, install the small copper insert, the NaI gamma-ray detector with preamplifier attached, and then the large copper housing. Add lead rings (7), (8), (9), (10), and (11). Finally, place the lead plug (P) on top of the shield and place the environmental chamber over the completed shield.

B. Equipment rack.

Place the RAMP system power supply on the top shelf of the equipment rack, passing the cables through the hole in the back of the shelf. Place the MCA on the center shelf and connect the cables from the NaI gamma-ray detector preamplifier to the "0 TO 1250 V POSITIVE H.V.," "PULSE INPUT," and "PREAMP POWER." Place the serial/parallel two-way converter to the left and to the back of the bottom shelf.

Hang the transmitter on the two screws on the back of the equipment rack. Connect the printer cable to the computer printer port. The other end of this cable is connected to the PARALLEL side of the serial/parallel two-way converter.

Connect a 25-pin RS232C cable to the SERIAL side of the serial/parallel two-way converter and to the 25-pin connector on the transmitter. Use tape to secure this cable to the back of the equipment rack.

Connect the 9-pin end of an RS232C cable to the computer, connect the other end of this cable to the 25-pin I/O Port RS232C on the MCA. Connect the antenna cable to the transmitter and the ARGOS antenna.

***** WARNING *****

The power switch on the back of the RAMP system power supply must be in the down (OFF) position and the ARGOS antenna connected to the transmitter before proceeding. The transmitter will be damaged if power is applied without a load on the antenna connector. Connect one end of the AC power cord to the inside of the environmental chamber, connect the other end to the multioutput AC extension box.

Connect the RED power plug from the RAMP system power supply to the computer.

Connect the BLACK power plug with the hole in the center from the RAMP system power supply to the MCA.

***** WARNING *****

Very carefully connect the BLACK miniature phone power plug from the RAMP system power supply to the serial/parallel two-way converter. It is possible to cause a short circuit and blow an internal fuse if this plug is not inserted properly.

Connect the AMP lock power connectors to the transmitter.

Connect the AC power cord of the RAMP system power supply to the multioutput AC extension box.

Power the RAMP system power supply with the switch on the back of the unit.

Power the MCA and perform setup as follows:

Press SETUP on the MCA.

Press the UP ARROW.

Press YES eight times or until BAUD RATE=9600 appears again.

Press the UP ARROW.

Press YES six times or until PARITY=8+NONE appears again.

Insert the SYSTEM DRIVE A disk into drive A on the right side of the computer.
Insert a formatted data disk into drive B on the left side of the computer.

Power the computer. The switch is toward the back on the right side. The computer will self-test, load, and execute "1RAMP," the RAMS control program.

The system is now ready for operation. Set the clock as described in Appendix A and perform the steps described in Appendix B. In the event of problems, go to Appendix C for system troubleshooting. Appendix D gives the schedule of routine operation.

3.4.4 EML QUALITY CONTROL

All data records being received from Service ARGOS are monitored by EML personnel daily to ensure that all sites are transmitting valid data. This includes almost continuous monitoring of EML VAX mail messages by EML personnel during the normal work day. All completed spectra received from Service ARGOS are also examined daily. Calibration spectra are computed and plotted as received. Background spectra are plotted and visually compared with previous background spectra. The results of the analyses of the sample spectra are examined for quality of fit and for the likelihood of fission products. The cause of excessively high quality of fit or fission product likelihood is determined, corrected, and a reanalysis is then performed.

All hard copy and computer files, both original data and results of analyses, are maintained at EML.

REFERENCES

- Larsen, R. J., H.-N. Lee, M. Monetti and C. G. Sanderson
"EML's Global Sampling Programs"
Proc. of the Conference on Atmospheric Chemistry, American Meteorological Society,
Boston, MA (1994)
- Sanderson, C. G., N. Latner and R. J. Larsen
"Environmental Gamma-Ray Spectrometry at Remote Sites with Satellite Data
Transmission"
Nuclear Instruments and Methods, A239, 271-277 (1994)
- Latner, N., C.G. Sanderson, V.C. Negro, S. Wurms and N. Chiu
"AUTORAMP - An Automatic Unit for Unattended Aerosol Collection, Gamma-Ray
Analysis and Data Transmission from Remote Locations"

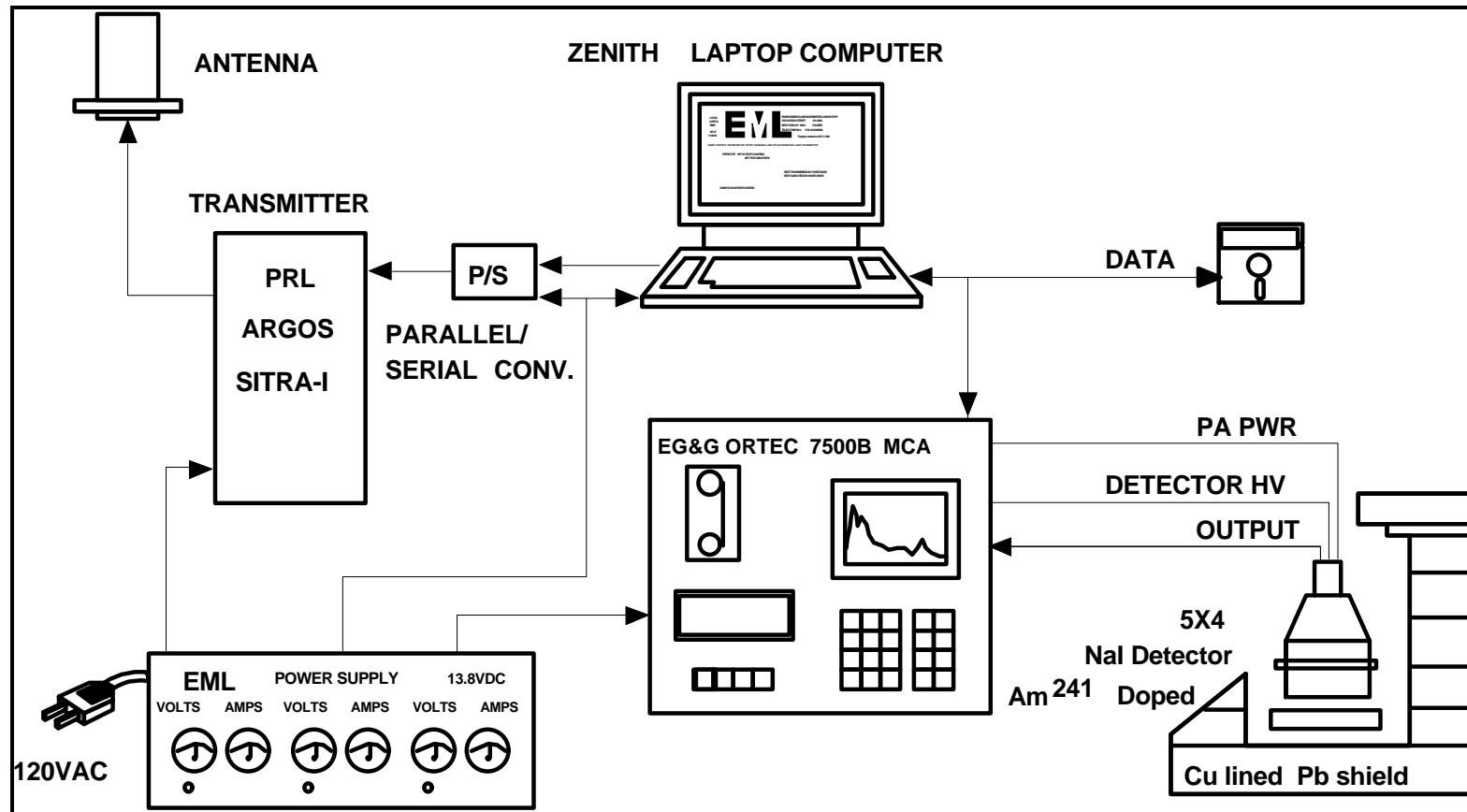


Figure 3.8. Block diagram of EML's second generation NaI RAMS.

Sylvia

APPENDIX A

OPERATION PROTOCOL

CONTROL PROGRAM MENUS

When the RAMP control program starts, there are four possible operations.

- I - for initial setup,*
- C - for system clock reset,*
- G - for MCA gain check, or*
- A - for data acquisition.*

INITIAL SETUP

Press the 'I' key on the computer. Enter the local date and time in the format as shown on the screen. Press ENTER. If the entry is correct, press the 'Y' key on the computer. If the entry is incorrect, press the 'N' key on the computer and reenter the correct local date and time.

If the 'Initial Setup' is entered in error, press the 'Q' key to quit this routine.

The default values displayed can be accepted by pressing ENTER. Press the 'Y' key to accept this value, or 'N' to enter a new value.

CLOCK RESET

It is very important that the date and time displayed in the upper-left corner of the screen is correct to within 1 h. If the date and time should change by more than 1 h, it must be reset. Press the 'C' key on the computer and enter the current local date and time

in the format as shown on the screen. Press ENTER. If the entry is correct, press the 'Y' key on the computer. If the entry is incorrect, press the 'N' key on the computer and reenter the correct local date and time.

DATA ACQUISITION - CALIBRATION

Press the 'A' key on the computer for data acquisition. When the 'A' key is pressed, there will be five possible operations.

- S - for sample count,*
- B - for background count,*
- C - for calibration count,*
- G - for MCA gain check, or*
- P - to return to previous menu.*

The first set of data obtained by the system must be a calibration count. Place a Coleman lantern mantle into the drawer of the RAMS counter and start data collection by pressing the 'C' key on the computer. The computer will automatically set up the analyzer and begin data collection. The calibration data should be collected for at least 4 h. Stop the calibration count by pressing the 'S' key, then the 'Y' key, and then the 'T' key. The calibration data will then be recorded on the floppy disk and transmitted to the ARGOS satellite. Remove the Coleman lantern mantle from the drawer of the RAMS counter.

DATA ACQUISITION - BACKGROUND

Press the 'A' key on the computer for data acquisition. When the 'A' key is pressed there will be five possible operations.

- S - for sample count,*
- B - for background count,*
- C - for calibration count,*
- G - for MCA gain check, or*
- P - to return to previous menu.*

Background data must be collected after the calibration and before any samples. Remove the Coleman lantern mantle from the drawer of the RAMS counter and replace with a BACKGROUND filter. Start data collection by pressing the 'B' key on the computer. The computer will automatically set up the analyzer and begin data collection. The background data should be collected at least overnight. Stop the background count by pressing the 'S' key, then the 'Y' key and then the 'T' key on the computer. The background data will then be recorded on the floppy disk and transmitted to the ARGOS satellite.

DATA ACQUISITION - SAMPLE

Press the 'A' key on the computer for data acquisition. When the 'A' key is pressed, there will be five possible operations.

- S - for sample count,*
- B - for background count,*
- C - for calibration count,*
- G - for MCA gain check, or*
- P - to return to previous menu.*

After one calibration and one background data set have been collected, exposed air filter samples can be counted.

Prepare for sample data collection by pressing the 'S' key. Enter the following information when requested on the computer screen.

- Date & time that sample collection started.
- Date & time that sample collection ended.
- Reading of running time meter when sample collection started.
- Reading of running time meter when sample collection ended.
- Reading of pressure meter when sample collection started.
- Reading of pressure meter when sample collection ended.
- Temperature when sample collection started.
- Temperature when sample collection ended.

Please refer to Appendix D for a schedule of when SAMPLES, CALIBRATIONS, and BACKGROUNDS should be counted.

When instructed, place the folded sample air filter into the drawer of the RAMS counter and start data collection by pressing any key on the computer. The computer will automatically set up the analyzer and begin data collection.

APPENDIX B

FIELD QUALITY CONTROL

POWER SUPPLY METERS

Each voltmeter should read about 14 V.

The MCA ammeter should read about 0.7 A with the display OFF and about 1.0 A with the display ON.

The laptop ammeter should read about 0.3 A with the display OFF and about 0.5 A when the display is ON.

The transmitter/converter ammeter should read about 0.3 A. Every 3 min when the transmitter is active this ammeter will read about 0.8 A for a second. This meter deflection is a good indication that the transmitter is operating.

LIGHT EMITTING DIODE (LED) INDICATORS

A red LED on the parallel/serial converter should be on, as it indicates the unit is powered.

A green LED on the MCA indicates that the battery is charging properly. If this LED should become red, a fault condition exists and EML must be notified by TELEX or FAX, but no operator action is required.

The three LEDs on the power supply should be on, as they indicate that the battery chargers are operating.

APPENDIX C

SYSTEM TROUBLESHOOTING

Once the system has been set up and is running, it should continue to do so indefinitely. There are a number of error traps built into the computer software program. If an error occurs and is trapped by the program, a message will be displayed indicating what action the operator should take.

Power for the transmitter/converter is protected with a 5 A internal fuse. If the LED on the serial/parallel two-way converter is not illuminated, and the transmitter/ converter meters indicate no voltage, this fuse may need to be replaced. In order to replace this fuse, the cover for the RAMP system power supply must be removed. The fuse holder is at the back of the left side of the unit. Spare fuses have been supplied with the backup equipment.

If none of the power supply LEDs are lit, the ammeters read 0 and the voltmeters read between 12 and 13 V, then the AC fuse at the back of the unit must be replaced to restore the AC (main) power. The batteries inside the power supply will continue to provide power for the RAMS for about 8 h.

If the computer does not respond, press 'CTRL,' 'ALT,' and 'DEL' at the same time. This will reset the computer and restart the program. Press the 'A' key, then either the 'C,' 'B' or 'S' key, as appropriate.

If the computer has entered the DOS operating mode as indicated by the DOS prompt A>, type 1RAMP and press ENTER to restart the program. Press the 'A' key, then either the 'C,' 'B' or 'S' key, as appropriate.

If the MCA has been turned off or has lost power for a long time, it will be necessary to reset the high voltage and to recycle the baud rate and parity so that communications with the computer can be established. Proceed as follows:

Press SETUP on the MCA.

Press the UP ARROW.

Press 'YES' eight times or until 'BAUD RATE=9600' appears again.

Press the UP ARROW.

Press 'YES' six times or until 'PARITY=8+NONE' appears again.

Press END.

Use 'CTRL,' 'ALT,' and 'DEL.' (This will reset the computer and restart the program.)

When the RAMP control program starts, there will be four possible operations.

I - for initial setup,

C - for system clock reset,

G - for MCA gain check, or

A - for data acquisition.

Press the 'I' key on the computer. Accept the default values displayed by pressing ENTER. Press the 'Y' key to accept these values. The high voltage will automatically be set to the correct value by the initial setup routine.

Computer software problems can develop if: 1) the MCA amplifier gain is beyond the range that the computer can correct; 2) the MCA gain setting when the unit was packaged for shipment was preset to an invalid value; and 3) the internal temperature of the environmental chamber was not set at 88°F. The MCA gain can be checked and adjusted as follows.

Press the 'G' key on the computer keyboard. "THE CURRENT GAIN VALUE IS" message will be displayed. After a few seconds, the current gain value will also be displayed. If the gain is very different from the preset value, enter the preset value and press the ENTER key on the computer. Press ENTER on the computer to leave the current gain value unchanged.

The MCA gain can also be reset automatically by the software. The procedure is as follows:

From the initial menu, press 'I' for initialization.

Enter the correct local date and time.

When prompted for a GAIN value, enter the word RESET.

Follow the instructions on the computer screen.

If the data that is being transmitted is not received by EML in New York City, EML will inform site operators by TELEX or FAX and ask operators to TELEX or FAX the status of the RAMS. After EML has determined the correct resolution of the problem, instructions will be communicated to site operators.

APPENDIX D

SCHEDULE FOR ROUTINE OPERATION

MONDAY - Transmit the SAMPLE count started on Friday by sequentially pressing the S, Y, and T keys on the computer.

Remove the exposed sample filter from the RAMP counter, write the date of transmission on the filter label under Notes, and mail the filter to the University of Miami.

Place the Coleman lantern mantle into the RAMP counter and start data collection by sequentially pressing the A and C keys on the computer.

WEDNESDAY - Transmit the CALIBRATION count started on Monday by sequentially pressing the S, Y, and T keys on the computer.

Remove the Coleman lantern mantle from the RAMP counter; store mantle.

Place the unexposed background filter into the RAMP counter and start data collection by sequentially pressing the A and B keys on the computer.

Change RAMP air filter and record pump data as outlined in Appendix A; store filter.

FRIDAY - Transmit the BACKGROUND count started on Wednesday by sequentially pressing the 'S', 'Y,' and 'T' keys on the computer.

Remove the unexposed background filter from the RAMP counter; store filter.

Fold and place the exposed filter sample collected on Wednesday into the RAMP counter and start data collection by pressing the 'A' and 'S' keys on the computer. Enter the data requested by the computer.

MONTHLY - At the end of each month, replace the data disk in Drive B of the computer and mail the old disk to EML.

3.5 THERMOLUMINESCENCE DOSIMETRY

Contact Person(s) : Gladys Klemic

3.5.1 SCOPE

Research at EML is directed toward advancements in environmental applications of thermoluminescence dosimetry (TLD). This includes investigations of problems associated with low-level measurements of the gamma- and cosmic-ray natural background (de Planque and Gulbin, 1985; Julius and de Planque, 1984; Gulbin and de Planque, 1983, 1984), as well as techniques for the separation of neutron and gamma components from artificial sources (Klemic et al., 1996). EML organizes the International Intercomparisons of Environmental Dosimeters, a voluntary program of testing and research on integrating dosimeters for the measurement of environmental radiation (Klemic et al., 1995; Maiello et al., 1990a,b, 1995; de Planque and Gesell, 1986) that attracts participants from around the world.

Consistent procedures for the preparation, packaging, recordkeeping and readout, along with many QC checks, are necessary to obtain reliable results. The procedures described here have been shown to result in high quality measurements that are suitable for low-level environmental radiation monitoring and for TLD research purposes (see also American National Standards Institute Report, ANSI N545-1975, and the future release of ANSI N13.37, which will replace it).

3.5.2 SPECIAL APPARATUS

1. TLD phosphors:

Lithium fluoride dosimeters - $^7\text{LiF:Mg,Ti}$ chips are used for most applications. They are 3.2 x 3.2 x 0.89 mm, 24 mg chips manufactured by Harshaw/Bicron Co., 6801 Cochran Rd., Solon, OH 44139-3395 (TLD-700).

Aluminum oxide dosimeters - $\text{Al}_2\text{O}_3\text{:C}$ chips are presently used only for research purposes. They are 5 mm in diameter and 1 mm thick and are manufactured by Victoreen, Inc., 6000 Cochran Rd., Solon, OH 44139-3395 (Model 2600-80).

Calcium fluoride chips and bulb dosimeters - EML's historical experience has included bulb-type dosimeters and other types of chips such as $\text{CaF}_2\text{:Mg}$ (Gulbin and de Planque, 1983; Gulbin and de Planque, 1984); however, these phosphors are not presently in use and will not be covered here.

2. Annealing equipment:

*High temperature furnace** - A furnace with constant temperature capability up to 1000°C (manufactured by Blue M Electric Co., Blue Island, IL 60406) is used for high temperature annealing.

Low temperature furnace - This furnace is maintained at 100°C for low temperature annealing (manufactured by Fisher Isotemp, Pittsburgh, PA 15219).

Planchet - An EML-designed, platinum-plated copper planchet is used for chip annealings. The tray is indented so that chips may be identified by placement (see Figure 3.9).

Brass heat sink - A brass heat sink, 5 x 5 x 21 cm, is mounted on an aluminum base that is placed on steel unistrut bars to allow uniform cooling of chips (see Figure 3.9).

3. Controlled lighting:

Gold fluorescent lights with no ultraviolet emissions.

Dark room shades.

Incandescent bulbs, including a 25-W red bulb for minimal lighting.

4. ^{137}Cs source:

A 2 Ci collimated NIST traceable ^{137}Cs source is used for calibration. Usual exposure distance is 2 m, where the beam is uniform within a radius of at least 3.0 cm.

*A new controlled atmosphere oven (manufactured by GS Lindberg/Blue M., Watertown, WI) has recently been installed for research but it is not yet in regular use.

5. TLD readers:

The TLD reader room is air-conditioned to maintain a constant temperature ($\sim 20^{\circ}\text{C}$) year-round. Three TLD readers are presently in use:

EML reader - This reader was built by EML and has been in use since 1971. It uses linear pan heating and measures the TL signal with a high-gain, low-noise photo-multiplier tube cooled to 15°C below room temperature. An internal light source is used to verify the electronic stability of the system. Power is applied to a heating element silver-soldered to a thin silver heater pan. The chip is positioned manually and centered in the pan by a removable platinum-plated, stainless-steel disk with a central hole for the TLD. This disk suppresses the infrared signal from the heater pan and provides a reproducible geometry for chip placement. Heating parameters are adjustable up to a maximum temperature of about 550°C . Purified nitrogen gas flows through the heating chamber at a rate of about 2.4 L min^{-1} to suppress any nonradiation induced TL signal. A strip chart records the glow curve and temperature profile with a selected glow peak region of interest indicated by pen offsets. The integral "counts" in this region is indicated on a numerical display.

Victoreen Model 2800M - A commercially available reader with many of the same features as the EML reader using updated technology, it will eventually replace the aging EML reader. Readout data can be sent to a printer or personal computer.

Automatic hot gas reader (TNO) - Built by Radiologische Dienst TNO at the Netherlands Organization for Applied Research, this reader is different from the other two, both in heating methods and chip handling. It uses three jets of preheated nitrogen gas (about 190°C constant temperature, not a linear profile) for reproducibility and speed. Chips are handled automatically at a rate of 150 per hour up to 1000 chip readings. Readout parameters and output are controlled and stored by a personal computer. This reader is especially suitable for large-scale studies and routine monitoring.

6. Lead shield:

A 10-cm thick lead shield is used to store TLDs after preparation or before readout.

3.5.3 PREDEPLOYMENT PREPARATION OF CHIPS

A. Batch preselection.

Before chips are to be used for measurements, a set (typically 200 to 300 chips) from a single manufacturing batch is tested for uniformity as follows:

1. Clean and anneal chips as described in Section B.
2. Give chips a single exposure to ^{137}Cs (typically on the order of $70\ \mu\text{Gy}$ in air, or 8 mR).
3. Read out the chips (see Table 1 for readout parameters).
4. Assign chips with readings that agree to within 30% of each other to the same group. Outliers should be flagged and removed from the group. (Note: A tighter criterion of 5-10% may be used for special applications.)
5. Assign each chip a unique identification number to be permanently retained.

B. Cleaning/annealing.

1. Manually clean individual chips before each use with methanol and a cotton swab, handling chips with forceps or a vacuum pen under appropriate lighting conditions (see Table 3.2) (Freeswick and Shambon, 1970).
2. Anneal chips as follows:
LiF: 1 h at 400°C , 1-min cool-down on heat sink, followed by 2 h at 100°C .
 Al_2O_3 : 10 min at 400°C .
3. Cool chips to room temperature on heat sink.
4. Store chips in the lead shield if they are not going to be used immediately. Keep careful records of the date and time that the chips are placed in the lead shield, as well as when they are removed for deployment.

C. Dosimeter packaging.

Packaging should be light-tight, moisture proof, and thick enough to provide electronic equilibrium and to shield against environmental beta radiation. The EML dosimeter consists of a commercially available black lucite box in which additional black lucite pieces have been bonded in place to provide depressions for holding the individual chips (see Figure 3.10). It has outside dimensions of 2.9 x 2.9 x 0.9 cm. Each chip is surrounded by lucite with a minimum thickness of 2.8 mm (about 320 mg cm⁻²). A dosimeter usually consists of five chips, though the container can hold up to 10 chips. To ensure water-tightness, the lucite box is placed inside a thin plastic bag which is heat sealed or secured with fiber tape.

3.5.4 ENVIRONMENTAL DEPLOYMENT

Environmental TLDs are usually deployed for 1-3 months. A preselected uniform batch (see Section 3.5.3.A) with enough TLDs to cover at least three monitoring cycles is maintained exclusively for use in environmental monitoring (i.e., while one set is in the field, there are enough dosimeters for two replacement sets). A set of environmental dosimeters for a monitoring cycle includes six control dosimeters prepared with the field dosimeters, as described in Section 3.5.3.B. All dosimeters are stored in the lead shield after preparation until they can be deployed, noting date and time. Two of the controls will be used to determine the exposure rate in this shield (STORAGE CONTROLS) and are thus stored there for the duration of the field cycle. The other four are used for calibration of the system (CALIBRATION CONTROLS) and will be discussed in Section 3.5.5.D.

If the field site is far from the laboratory, it is necessary to use additional controls to account for exposure received in transit (TRANSIT CONTROLS). These controls must be kept with the field dosimeters at all times except during field deployment, when they must be kept somewhere where the exposure rate is known or can be measured independently.

The dosimeter is hung 1 m above the ground, away from large structures that may provide shielding or additional exposure (see Figure 3.11). Usually the dosimeter is left hanging freely to rotate in the wind for isotropic angular exposure. At the end of the field cycle, the dosimeters are returned to the lead shield until they are read out, and a replacement set is deployed in the field.

3.5.5 READOUT AND CALIBRATION

A. Reader checkout.

1. Prepare the reader for use by setting the appropriate reader parameters as shown in Table 3.2.
2. Check the reader's dark current, the heating chamber current (background of empty chamber), and the response of the reader to the internal light source.
3. Read out a test chip several times to check for anomalous results.

B. Preread annealing.

1. Remove the FIELD dosimeters from the lead shield, noting the date and time.
2. Perform a preread anneal for LiF chips at 100°C for 10 min. (No preread anneal is used for Al₂O₃ chips.)

C. Initial readout.

1. Read out **one** chip from each FIELD dosimeter. After it returns to room temperature, the chip is read a second time to measure the background of the system.
2. Temporarily discontinue readout at this point to prepare the calibration dosimeters.

D. Calibration.

Four dosimeters are used to calibrate the system during readout. Two of these are from the set originally prepared at the start of the field cycle, and two are taken from the set of replacement dosimeters just prepared. Thus, while each prepared set includes four calibration dosimeters, two will be used right away to calibrate the returning field set and the other two are stored in the lead shield for the duration of the field cycle to be used at the following readout. The calibration is performed as follows:

1. Examine the range of reader net counts from the initial readout of each field dosimeters to determine the calibration exposures to use. Choose three calibration exposures to bracket the readings given by the field dosimeters and to provide a check on the linearity of the system. (The approximate counts per unit exposure is known from previous readouts.)
2. Remove the CALIBRATION CONTROLS from the lead shield, noting the date and time of retrieval.
3. Give one CALIBRATION CONTROL an exposure that is expected to yield net counts in the range of the lowest result found for the FIELD dosimeters. Another CALIBRATION CONTROL is given an exposure corresponding to the highest reading, and the other two receive an exposure in the middle of this range.

E. Resuming readout.

1. Remove the STORAGE CONTROL dosimeters from the lead shield, noting the date and time.
2. Anneal all of the control dosimeters in the case of LiF TLDs (the four CALIBRATION CONTROLS as well as the two STORAGE CONTROLS) for 10 min at 100°C.
3. Intersperse the STORAGE CONTROL and CALIBRATION CONTROL dosimeters among the FIELD dosimeters. Read out one chip from each dosimeter before going to the next chip in any dosimeter. (This provides a QC check against any variations in the system during readout.)

3.5.6 ANALYSIS OF RESULTS

An interactive program that runs on a personal computer (written in Fortran) handles the data analysis. A sample input file is shown in Appendix A. It includes for each dosimeter: date and times of preparation, deployment, return, and readout; gross counts; background counts; and time of exposure to the cesium source. The program determines the field exposure by correcting for exposure received in storage as measured by the

storage controls and then converting counts to exposure by using the calibration controls. The user is given the option of rejecting outliers, and the statistical error is propagated throughout each step in the calculation. The program returns the net field exposure and exposure rate and the field deployment time for each field dosimeter. It also gives information about the exposure rate in storage, the calibration factor, and any rejected readings. A sample output file is shown in Appendix A. Details of the calculations are given below.

A. Computing net counts and standard error.

The mean net counts for each dosimeter is:

$$\bar{X} = \sum_{i=1}^n (x_i) \div n$$

where

x_i = gross counts - background counts of i th chip.

n = number of chips per dosimeter ($n = 5$ usually).

The standard error of the mean for each dosimeter is:

$$\text{err}_x = \frac{\sigma}{\sqrt{n}} = \sqrt{\frac{\sum_{i=1}^n (x_i - \bar{X})^2}{n(n-1)}}$$

B. Outlier check.

The program checks for outliers among the individual chip readings in a dosimeter. Two different criteria are used:

1. "*Extreme Values*" - Individual chip net counts that are $> 150\%$ or $< 50\%$ of the dosimeter average \bar{X} are flagged. This test would find missing chips or noise spikes.

2. *"r Test"* - This is an outlier test for gaussian distributions (Proschan, 1969). The net counts for the five chips are ranked in order of smallest to the largest, such as x_1, x_2, x_3, x_4, x_5 . If the ratio $r = (x_2 - x_1) \div (x_5 - x_1)$ is larger than 0.780, chip x_1 is flagged. Similarly if the ratio $r = (x_5 - x_4) \div (x_5 - x_1)$ is larger than 0.780, chip x_5 is flagged. This is a more sensitive test that can identify outliers that would be missed by the extreme value test. While it is redundant for values beyond 150% of the mean, it could miss the very low extreme values so both tests are needed. (Proschan describes more sensitive tests to apply when more than 7 chips are used.)

In either criterion, the user is then given the option of omitting flagged chips from the analysis. No chips are automatically rejected: the final decision is made by the user. (In practice data are rarely rejected, and then usually for obvious reasons.) If a chip is rejected, the mean net counts and standard error are recalculated for that dosimeter, and a note appears in the output file.

C. Storage exposure rate correction factor.

$$S = (1/2)(X_{SC1} + X_{SC2}) \div t_{SC}$$

where

- S = storage correction factor,
- X_{SC1} = mean net counts for STORAGE CONTROL #1,
- X_{SC2} = mean net counts for STORAGE CONTROL #2, and
- t_{SC} = time storage controls were in lead shield (*calculated by subroutine from dates in input file*)

The standard error is propagated through this calculation as:

$$\text{err}_S = \frac{1}{2t_{SC}} \sqrt{(\text{err}_{SC1}^2 + \text{err}_{SC2}^2)}$$

With err_{SC1} and err_{SC2} being the standard error of the storage controls as defined in Section A above. (The error associated with the storage time is negligible, estimated at < 0.01%.)

D. Calibration factor.

$$C = \left(\frac{1}{4} \right) \sum_{i=1}^4 (X_{CCi} - S t_{CCi}) \div \text{exposure}_{CCi}$$

where

C = calibration factor,

X_{CCi} = mean net counts of CALIBRATION CONTROL # i

t_{CCi} = time i th CALIBRATION CONTROL was kept in lead shield (*calculated by subroutine from dates in input file*),

exposure_{CCi} = cesium exposure given to i th CALIBRATION CONTROL (*calculated from decay corrected known source strength and time of exposure*).

The standard error propagated through this calculation is then:

$$\text{err}_C = \frac{1}{4} \sqrt{\sum_{i=1}^4 \left(\frac{\text{err}_{CCi}^2 + \text{err}_S^2 t_{CCi}^2}{\text{exposure}_{CCi}^2} \right)}$$

(Uncertainties in cesium calibration exposure are treated as systematic rather than statistical errors and are treated separately.)

The program also performs a linear regression on the corrected counts vs. exposure for the four calibration dosimeters. The goodness of fit is a check on the linearity of the system and the slope may be compared to C .

E. Field exposure.

The field site exposure (f) is a function of the quantities calculated above. The algorithm used by the program to calculate field site exposure may be summarized as:

$$F = f(X_F, t_F, S, C) = \frac{(X_F - S t_F)}{C}$$

where

X_F = mean FIELD dosimeter counts

t_F = time FIELD dosimeters were kept in a lead shield (*calculated by subroutine from dates in input file*),

F. Error analysis.

Total uncertainty = statistical error at 95% confidence + estimated systematic error

While the standard error was propagated through all the above calculations using the analytical propagation of error formulas, for the last step it is easier to calculate the statistical error numerically as shown below (Bevington and Robinson, 1992).

$$\text{Statistical err} = 2.776 \sqrt{(a^2 + b^2 + c^2)}$$

where

2.776 = 95% confidence interval for 5 chips
(4 degrees of freedom)

$$a = \frac{([X_F + \text{err}_F] - S t_F)}{C} - \frac{(X_F - S t_F)}{C}$$

$$b = \frac{(X_F - (S + \text{err}_F) t_F)}{C} - \frac{(X_F - S t_F)}{C}$$

$$c = \frac{(X_F - S t_F)}{(C + \text{err}_C)} - \frac{(X_F - S t_F)}{C}$$

Systematic error is estimated on a case-by-case basis and added linearly to the statistical error for reporting the final results. The estimated systematic uncertainty associated with EML's cesium source is 2.5%.

G. Situations involving transit controls.

In cases where TRANSIT CONTROLS are required, the field exposure (Section E) calculation would instead be:

$$F = (X_F - T)/C$$

where

T = mean TRANSIT dosimeter counts corrected for exposure received in storage.

If it happens that the TRANSIT CONTROLS are stored in the same lead shield as the other storage controls during the field cycle (time = t_F), then

$$T = (X_T - S t_F)$$

where

X_T = mean TRANSIT dosimeter counts.

More likely the TRANSIT CONTROLS will be stored in a different lead shield near the field site, in which case the storage exposure must be measured by some other means.

REFERENCES

"American National Standard Performance, Testing, and Procedural Specifications for Thermoluminescence Dosimetry (Environmental Applications)"
American National Standards Institute Report, ANSI N545-1975 (1975)

Bevington, P. R. and D. K. Robinson

"Data Reduction and Error Analysis for the Physical Sciences"
Second Edition, McGraw-Hill, Inc., New York, p. 49 (1992)

de Planque, G. and T. F. Gesell

"Environmental Measurements with Thermoluminescence Dosimeters - Trends and Issues"

Radiation Protection Dosimetry, 17, 193-200 (1986)

de Planque, G. and J. F. Gulbin

"The Effects of Moisture on LiF TLDs and Its Consequences for Environmental Measurements"

Proceedings 18th Midyear Health Physics Symposium, pp. 307-315, January (1985)

Freeswick, D. C. and A. Shambon

"Light Sensitivity of LiF Thermoluminescent Dosimeters"

Health Physics, 19, 65 (1970)

Gulbin, J. F. and G. de Planque

"An Investigation of Field Fading in LiF (TLD-700) in an Environmental Monitoring Program"

Radiation Protection Dosimetry, 5, 155-199 (1983)

Gulbin, J. F. and G. de Planque

"Ten Years of Residential TLD Monitoring"

Radiation Protection Dosimetry, 6, 299-303 (1984)

Julius, H. W. and G. de Planque

"Influence of Annealing and Readout Procedures on Fading and Sensitivity Changes in LiF for Temperatures and Humidities Typical for Environmental and Personnel Dosimetry"

Radiation Protection Dosimetry, 6, 253-256 (1984)

Klemic, G.A., N. Azziz and S.A. Marino

"The Neutron Response of $\text{Al}_2\text{O}_3\text{:C}$, $^7\text{LiF:Mg, Cu, P}$, and $^7\text{LiF:Mg, Ti}$ TLDs"

Radiation Protection Dosimetry, 65, 221-226 (1996)

Klemic, G.A., J. Shobe, T. Gesell and P. Shebell

"Results of the Tenth International Intercomparison of Environmental Dosemeters"

Radiation Protection Dosimetry, 58, 133-142 (1995)

Maiello, M., J. F. Gulbin, G. de Planque and T. F. Gesell

"8th International Intercomparison of Environmental Dosimeters"

Radiation Protection Dosimetry, 32, 91-98 (1990a)

Maiello, M., J. F. Gulbin, G. de Planque, and H. Thompson Heaton

"Ninth International 'Mini' Intercomparison of Environmental Dosemeters: A Further
Analysis of the Data"

Radiation Protection Dosimetry, 58, 167-175 (1995)

Proschan, F.

in: *Precision Measurement and Calibration*

Ku, H. H. (ed.)

Selected NBS Papers on Statistical Concepts and Procedures

NBS Special Publication 300, Vol. 1, pp. 349-354 (1969)

TABLE 3.2

SUMMARY OF TLD PARAMETERS USED

ANNEALING		
	Predeployment	Prereadout
LiF	400°C 1 h 100°C 2 h	100°C 10 min
Al ₂ O ₃	400°C 10 min	none

LIGHTING CONDITIONS	
LiF	no UV: gold fluorescent or incandescent
Al ₂ O ₃	darkroom

READ OUT Linear Heating: Victoreen Reader				
	Starting Temp	Heating Rate	Heating Time	Integration Period*
LiF	100°C	10°C sec ⁻¹	30 sec	~ 10 - 20 sec
Al ₂ O ₃	100°C	10°C sec ⁻¹	20 sec	~ 5 - 20 sec

Table 3.2 (Cont'd)

READ OUT Linear Heating: EML			
	Heating Rate	Maximum Temperature	Integration Period* (adjusted visually)
LiF	10°C sec ⁻¹	~ 330°C	peaks 3,4 &5
Al ₂ O ₃	10°C sec ⁻¹	~ 300°C	whole peak

READ OUT Constant Temperature Hot Gas: TNO		
	Heating Time	Integration Period*
LiF	11 sec	1.3 - 10.0 sec
Al ₂ O ₃	13 sec	1.7 - 12.0 sec

*Integration period adjusted as needed to include entire peak.



Figure 3.9. EML-designed planchet used for chip annealings, shown on brass heat sink. Chip identity is retained by position in planchet.

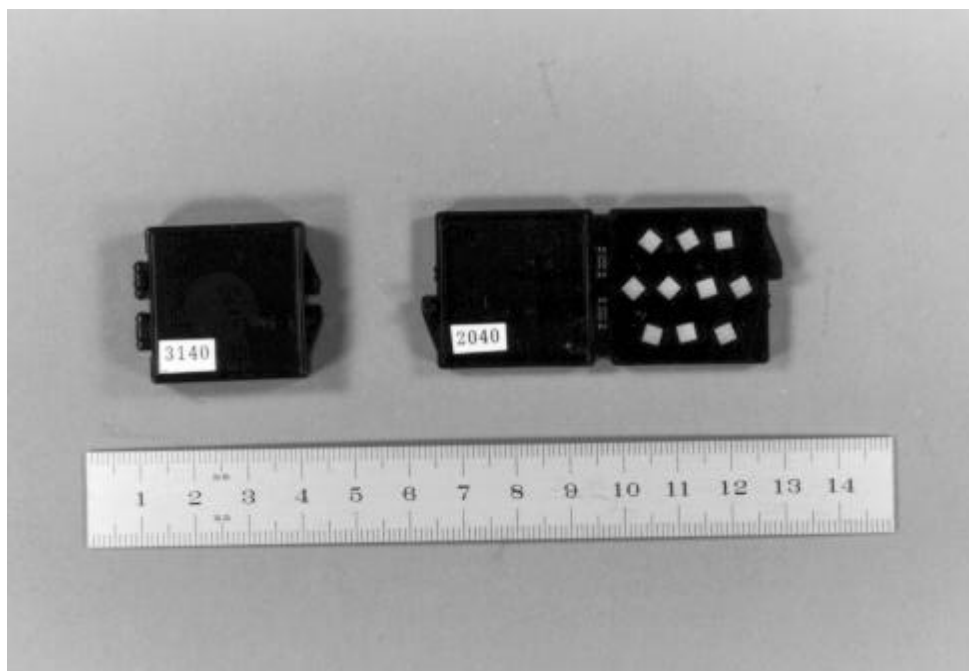


Figure 3.10. EML's light-tight lucite dosimeter package (320 mg cm^{-2}), shown here in closed and open positions with 10 LiF chips.

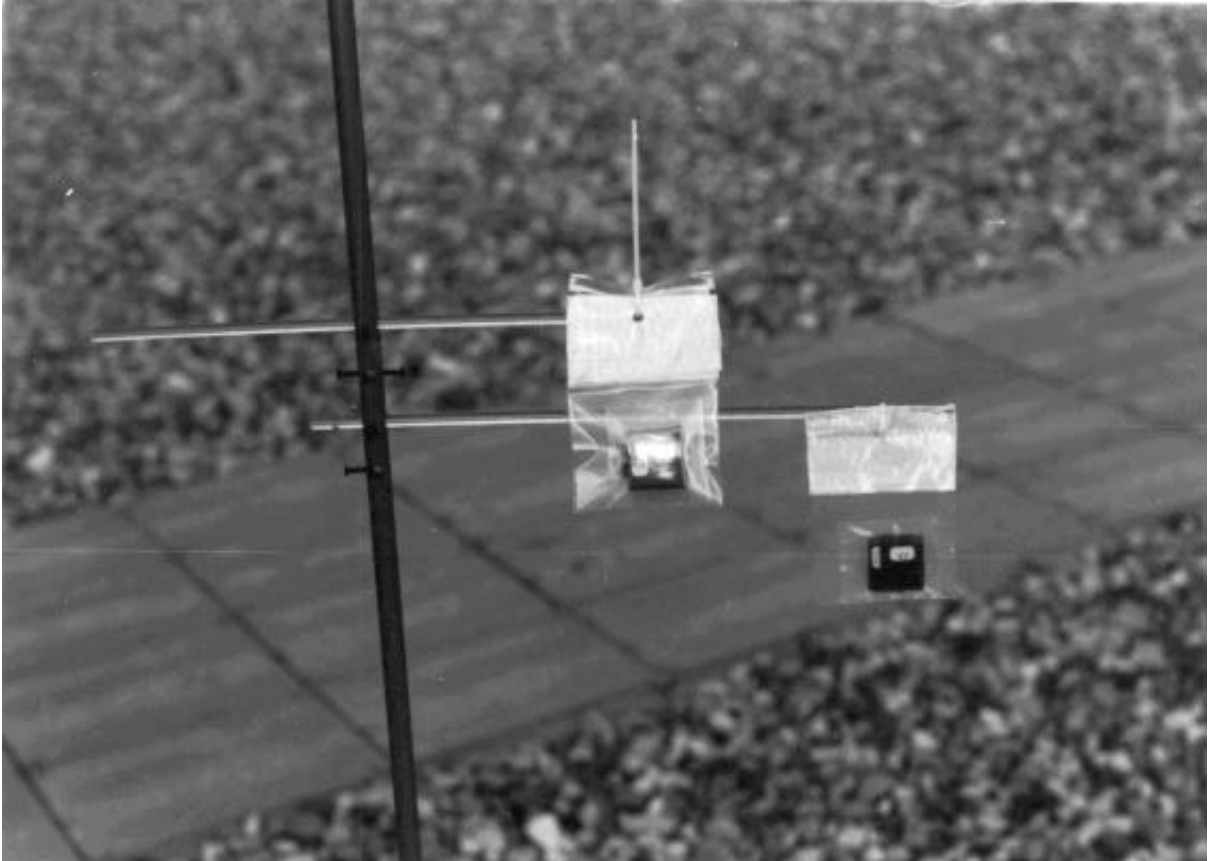


Figure 3.11. EML dosimeter deployed at field site. Lucite box is sealed in plastic bag to protect from moisture, and hung ~ 1 m above ground.

APPENDIX A

SAMPLE INPUT FILE Environmental TLD Measurements

SITE	ID	INTO LEAD	DEPLOYED	RET. LEAD	READ OUT	Counts		Cs Expos min
		SHIELD		SHIELD		GROSS	BKD	
Shrm	3140	02/21/93 19:23	02/26/93 15:55	04/27/93 07:37	10/20/93 09:45	430	36	0.00
						425	32	
						417	34	
						414	30	
						447	38	
Roof	3100	02/21/93 19:23	03/01/93 15:20	05/25/93 12:45	10/20/93 09:45	534	35	0.00
						507	33	
						556	28	
						536	36	
						550	36	
Chstr	3110	02/21/93 19:23	02/23/93 14:45	05/19/93 12:00	10/20/93 09:45	808	29	0.00
						812	36	
						806	29	
						803	30	
						783	34	
Chstr	3120	02/21/93 19:23	02/23/93 14:45	05/19/93 12:00	10/20/93 09:45	811	30	0.00
						802	30	
						764	34	
						739	38	
						764	33	
Sphr	3130	02/21/93 19:23	03/01/93 15:20	05/25/93 12:45	10/20/93 09:45	319	35	0.00
						349	31	
						333	30	
						338	30	
						347	31	
Stor Ctl	3200	02/21/93 19:23	00/00/00 00:00	00/00/00 00:00	10/20/93 09:45	265	29	0.00
						257	32	
						264	27	
						267	32	
						253	29	
Stor Ctl	3190	02/21/93 19:23	00/00/00 00:00	00/00/00 00:00	10/20/93 09:45	241	32	0.00
						269	36	
						329	32	
						244	32	
						239	32	
Calib 1	3150	02/21/93 19:23	00/00/00 00:00	00/00/00 00:00	10/20/93 09:45	478	31	3.50
						511	32	
						471	35	
						489	39	
						486	36	
Calib 2	3160	02/21/93 19:23	00/00/00 00:00	00/00/00 00:00	10/20/93 09:45	656	31	6.0
						643	30	
						675	34	
						618	41	
						643	34	
Calib 3	3000	04/23/93 13:00	00/00/00 00:00	00/00/00 00:00	10/20/93 09:45	614	30	6.0
						598	34	
						610	32	
						666	38	
						597	30	
Calib 4	3050	04/23/93 13:00	00/00/00 00:00	00/00/00 00:00	10/20/93 09:45	771	28	9.0
						798	31	
						791	32	
						777	32	
						796	29	

APPENDIX A (Cont'd)

SAMPLE OUTPUT FILE

Environmental TLD Measurements (with statistical uncertainty at 1 σ)

<u>SITE</u>	<u>DEPLOYMENT</u>		<u>NETmR</u>	<u>EXPOSURE RATE μR/h</u>	<u>FIELD h</u>
Shrm	2-26-93	4-27-93	9.12	6.37 \pm .25 (3.9%)	1431.70
Roof	3-01-93	5-25-93	14.53	7.13 \pm .22 (3.1%)	2037.42
Chstr	2-23-93	5-19-93	24.68	12.11 \pm .29 (2.4%)	2037.25
Sphr	3- 1-93	5-25-93	6.73	3.30 \pm .17 (5.2%)	2037.42

Stor. Corr. Factor: .0448 \pm .00150 cts/h (3.4%)

Ave. Calibration Factor: 25.028 \pm .428 cts/mR (1.7%)

Lead Shield Exp. Rate: 1.789 \pm .067 micro-R/h (3.8%)

<u>SITE</u>	<u>SN</u>	<u>Net Cts</u>	<u>Store h</u>	<u>Cor. Cts</u>	<u>err</u>	<u>% err</u>	<u>sd</u>	<u>%sd</u>
Shrm	3140	422.60	4342.67	228.19	\pm 8.0	(1.1%)	10.5	4.58
Roof	3100	531.00	3736.95	363.71	\pm 9.5	(1.5%)	17.3	4.75
Chstr	3110	784.90	3737.12	617.60	\pm 10.0	(1.1%)	26.3	4.26
Sphr	3130	335.80	3736.95	168.51	\pm 8.3	(1.8%)	13.6	8.08
Stor Ctl	3200	255.40	5774.34	255.40	\pm 3.4	(1.3%)	7.5	2.94
Stor Ctl	3190	261.60	5774.34	261.60	\pm 17.0	(6.5%)	38.0	14.53
Calib 1	3150	482.40	5774.34	223.90	\pm 11.2	(1.5%)	15.9	7.12
Calib 2	3160	645.00	5774.34	386.50	\pm 12.5	(1.4%)	20.0	5.17
Calib 3	3000	614.20	4316.72	420.95	\pm 13.2	(1.9%)	25.8	6.13
Calib 4	3050	782.20	4316.72	588.95	\pm 8.8	(0.8%)	13.3	2.26

APPENDIX A (Cont'd)

SAMPLE OUTPUT FILE continued

.....CALIBRATION INFORMATION.....

<u>Name</u>	<u>SN</u>	<u>Expos mR</u>	<u>cts/mR</u>	<u>err</u>	<u>%err</u>
Calib 1	3150	9.229	24.260	± 1.216	(5.0%)
Calib 2	3160	15.821	24.429	± 0.787	(3.2%)
Calib 3	3000	15.821	26.607	± 0.836	(3.1%)
Calib 4	3050	23.732	24.817	± 0.371	(1.5%)

Fit to line:

slope = 25.084 (cts/mR)
y intercpt = -0.05930
rnorm = 28.031
ierr = 0

The following packets had outlier data rejected:

(none)

3.6 BONNER-SPHERE NEUTRON SPECTROMETRY

Contact Person(s) : Paul Goldhagen

3.6.1 SCOPE

Described here are EML's moderated multisphere neutron spectrometers, also known as Bonner sphere neutron spectrometers, and the general principles of their use in neutron spectrometry. These spectrometers are used to measure neutron fields:

1. That result from cosmic-ray interactions in the atmosphere (Hajnal et al., 1971; Nakamura et al., 1987);
2. In the containment of pressurized nuclear reactors (Hajnal et al., 1979; Nakamura et al., 1984; Sanna et al., 1980);
3. Around unmoderated (fast) reactors (Griffith et al., 1984; Hoots and Wadsworth, 1984).
4. In plutonium facilities (Harvey and Hajnal, 1993).
5. Fusion test reactors (Kugel et al., 1994a,b).

3.6.2 GENERAL DESCRIPTION

The primary Bonner sphere spectrometer system consists of 12 moderated polyethylene spheres equipped with boron-trifluoride proportional counters. The spectrometers are usable either in parallel or in the independent mode. In the parallel mode, all the spheres are exposed simultaneously to the neutron field, while in the independent mode they are exposed sequentially. Sufficient detail is given here for the basic methodology; the references cited should be consulted for additional information (Aldrich et al., 1981; Awschalom and Sanna, 1985; Cross and Ing, 1987).

At EML, neutron spectrometry is carried out on an occasional basis, usually to answer specific research requirements or questions. Consequently, there are not rigidly defined procedures. Considerable expertise and judgement are required to perform Bonner sphere spectrometry, and this section should be considered as a guide rather than a specific procedure.

3.6.3 PERSONNEL AND TRAINING

The procedures described in this section should be conducted and/or supervised by an experienced physicist or nuclear engineer and that individual should be thoroughly familiar with the content of the references cited in this section.

3.6.4 METHODOLOGY

3.6.4.1

DESCRIPTION OF THE SYSTEM

Bonner sphere spectrometers have been used extensively in radiation protection practices to determine neutron spectral distributions around particle accelerators, nuclear power stations and other nuclear facilities, as well as in cosmic-ray neutron research for over two decades. The Bonner sphere spectrometer system is very useful since it is simple, portable, has an isotropic response, covers a wide energy range, and the data can be unfolded and interpreted fairly easily (Bramblett et al., 1960).

One drawback of this method is the low energy resolution. This is partially due to the fact that the statistical fluctuations in the number of collisions in the neutron slowing down processes are large, and the capture reactions are completely indistinguishable from one another. This results in loss of information about the primary neutron energy and, consequently, low resolution.

3.6.4.2

THE BONNER SPHERES

The 12 Bonner spheres are: one bare and one 0.075-cm Cd covered 5.08-cm diameter boron-trifluoride spherical proportional counter, and 10 spherical polyethylene moderators of 7.62-cm, 7.85-cm, 10.01-cm, 10.24-cm, 12.75-cm, 14.94-cm, 15.24-cm, 19.96-cm, 25.04-cm and 30.07-cm diameters, respectively, with spherical proportional counters placed at the centers.

3.6.4.3

THE RESPONSE FUNCTIONS

The Bonner sphere spectrometer response functions must be calculated. The calculations should be performed using different numerical methods (such as those incorporated in the ANISN and MORSE codes), different evaluated neutron cross section sets, and different energy binning. The response functions of the boron-trifluoride counter equipped Bonner spheres are calculated using DTF-IV and by ANISN transport codes in the adjoint mode. The calculated detector response functions are considered sufficiently accurate if the results obtained using different cross section sets and transport codes differ by only a few percent for the entire energy region (Burgart and Emmett, 1972; Maerker et al., 1971).

3.6.4.4

CALIBRATIONS

The Bonner sphere spectrometer calibrations, whenever possible, should be performed with the National Institute of Standards and Technology (NIST) monoenergetic neutron beams, and the normalization of the overall response functions should be performed using ^{252}Cf spontaneous fission neutron sources. At EML, the ^{252}Cf calibrations are performed in an open air calibration facility, where the air and ground scattering contribution in the worst case amounts to only 3% at 1 m source-to-detector separation (Hajnal et al., 1970; Hunt, 1984a,b).

3.6.4.5

ELECTRONICS

Since the boron-trifluoride counters are not sensitive to β or γ radiation, a simple electronic setup is sufficient: a proportional counter is connected to a preamplifier and the signal is fed to a linear amplifier, followed by a discriminator and a scaler to record the number of capture reactions. The scaler readouts can be recorded on tape, or in an appropriate logbook.

3.6.5 NEUTRON SPECTRUM UNFOLDING

The result of a set of measurements with Bonner spheres is a set of 12 count rates for the 12 detector configurations. A mathematical method known as unfolding is used to obtain a neutron spectrum from these data. This is accomplished using a computer program entitled TWOGO developed at EML (Hajnal, 1981).

The relative count rates obtained for a set of 12 counts made with the Bonner spheres are a function of the energy distribution of the neutron field. The unfolding code provides a reasonable estimate of neutron fluence rate as a function of energy, i.e., a neutron spectrum (Ing and Makra, 1978). The user of TWOGO provides an estimate of the shape, called trial vector, of the neutron spectrum and the computations performed by TWOGO iteratively adjust the spectrum to fit or be consistent with the data. The computations rely on the use of the data available in the literature regarding the response of the detector in its various configurations, as a function of neutron energy. Estimates of the relative errors of individual counts are used as weighting factors during the iterative fitting process.

Several indices are computed with the TWOGO program that serve to measure the goodness of fit of the unfolding process. These indices are based on determining the degree of agreement between the data obtained by observation. That is, count rates due to neutrons for each of the detector configurations, and synthetic counts or estimates of these same parameters obtained by folding together the response matrix and the spectrum obtained by the unfolding process.

3.6.6 ACCEPTABLE SOLUTION

A solution can be called exact, approximate, or appropriate (Gold, 1964). Exact solutions may have zero errors, and might look reasonable. However, they may have unphysical characteristics, such as oscillations, and the "tail-wags-the-dog syndrome" might appear. Usually, the unfolded data should not be expected to have too good a fit, at least not better than the error of the input data. In general, the trial vectors should contain the features of the neutron spectra one can expect from the physics of the problem. Similarly, the smoothing functions, if any, have to be properly chosen. Appropriate solutions can be obtained from good measurements, and considerable experience is needed to judge just when a reasonable spectral solution is reached.

REFERENCES

Aldrich, J. M., D. L. Haggard, G. W. R. Endres, J. J. Fix, F. M. Cummings,
M. R. Thorson and R. L. Kathren
"Evaluating Existing Radiation Fields"
Pacific Northwest Laboratory Report PNL-3536, Richland, WA (1981)

Awschalom, M. and R. S. Sanna
"Application of Bonner Sphere Detectors in Neutron Field Dosimetry"
Radiation Protection Dosimetry, 10, 89 (1985)

Bramblett, R. L., R. I. Ewing and T. W. Bonner
"A New Type of Neutron Spectrometer"
Nuclear Instruments and Methods, 9, 1 (1960)

Burgart, C. E. and M. B. Emmett
"Monte Carlo Calculations of the Response Functions of Bonner Ball Neutron
Detectors"
Oak Ridge National Laboratory Report ORNL-TM-3739, Oak Ridge, TN (1972)

Cross, W. G. and I. Ing
"Neutron Spectrometry"

In: The Dosimetry of Ionizing Radiation

Kase, K. R., B. E. Bjarngard and F. A. Attix (Editors)

Academic Press, Vol. II, pp. 91-169, Orlando, FL (1987)

Gold, R.

"An Iterative Unfolding Method for Response Matrices"

USAEC Report ANL-6984, Argonne National Laboratory, Argonne, IL (1964)

Griffith, R. V., C. J. Huntzinger, and J. H. Thorngate

"Neutron Spectra as a Function of Angle at Two Meters from the Little Boy
Assembly"

Lawrence Livermore National Laboratory Report UCRL-90178, Livermore, CA (1984)

Hajnal, F.

"An Iterative Nonlinear Unfolding Code: TWOGO"

USDOE Report EML-391 (1981)

Hajnal, F., J. E. McLaughlin and R. Oeschler

"Technique for Determining Moderated-Neutron Instrument Characteristics"

USAEC Report HASL-222 (1970)

Hajnal, F., J. E. McLaughlin, M. S. Weinstein and K. O'Brien

"Sea-Level Cosmic-Ray Neutron Measurements"

USAEC Report HASL-241 (1971)

Hajnal, F., R. S. Sanna, R. M. Ryan and E. H. Donnelly

"Stray Neutron Fields in the Containment of PWRs"

International Atomic Energy Agency Report IAEA-SM-242/24, STI/PUB/527,
Vienna (1979)

Harvey, W. F. and F. Hajnal

"Multisphere Neutron Spectroscopy Measurements at the Los Alamos National
Laboratory Plutonium Facility"

Radiation Protection Dosimetry, 50, 13-30 (1993)

Hoots, S. and D. Wadsworth

"Neutron and Gamma Dose and Spectra Measurements on the Little Boy Replica"

Lawrence Livermore National Laboratory Report UCRL-90095, Livermore, CA (1984)

Hunt, J. B.

"The Calibration of Neutron Sensitive Spherical Devices in Non-Isotropic Neutron Fields"

Radiation Protection Dosimetry, 9, 105 (1984a)

Hunt, J. B.

"The Calibration of Neutron Sensitive Spherical Devices"

Radiation Protection Dosimetry, 8, 239 (1984b)

Ing, H. and S. Makra

"Compendium of Neutron Spectra in Criticality Accident Dosimetry"

International Atomic Energy Agency Report, IAEA Technical Report Series No. 180, Vienna (1978)

Kugel H. W., G. Ascione, S. Elwood, J. Gilbert, L. P. Ku, J. Levine, K. Rule,
N. Azziz, P. Goldhagen, F. Hajnal and P. Schebell

"Measurements of TFTR D-T Radiation Shielding Efficiency"

in: Fusion Engineering and Design, Proceedings of the Third International Symposium
of Fusion Nuclear Technology, Los Angeles, CA., September (1994a)

Kugel, H. W., J. Gilbert, D. Hwang, M. Lewis, J. Levine, L. P. Ku, K. Rule,
F. Hajnal, N. Azziz, P. Goldhagen, G. Klemic and P. Shebell

"TFTR Radiation Contour and Shielding Efficiency Measurements During D-D
Operations"

in: Fusion Technology, Proceedings of the Eleventh Topical Meeting on the Technology
of Fusion Energy, American Nuclear Society, September (1994b)

Maerker, R. E., L. R. Williams, F. R. Mynatt and N. M. Greene

"Response Functions for Bonner Ball Neutron Detectors"

Oak Ridge National Laboratory Report ORNL-TM-3451, Oak Ridge, TN (1971)

Nakamura, T., T. Kosako and S. Iwai

"Environmental Neutron Measurements Around Nuclear Facilities with Moderated-Type Neutron Detector"

Health Physics, 47, 729 (1984)

Nakamura, T., Y. Uwamino, T. Ohkubo and H. Hara

"Altitude Variation of Cosmic Ray Neutrons"

Health Physics, 53, 509 (1987)

Sanna, R. S., F. Hajnal, J. E. McLaughlin, J. F. Gulbin and R. M. Ryan

"Neutron Measurements Inside PWR Containments"

USDOE Report EML-379 (1980)